Unifying kinetic approach to phoretic forces and torques onto moving and rotating convex particles

Unifying kinetic approach to phoretic forces and torques onto moving and rotating convex particles

Martin Kröger[a)] and Markus Hütter[b)]
Polymer Physics, ETH Zürich, Department of Materials, Wolfgang-Pauli-Strasse 10, CH-8093 Zürich, Switzerland

(Received 1 March 2006; accepted 2 June 2006; published online 26 July 2006)

We derive general expressions and present several examples for the phoretic forces and torques acting on a translationally moving and rotating convex tracer particle, usually a submicrosized aerosol particle, assumed to be small compared to the mean free path of the surrounding nonequilibrium gas. Point of departure is an expression of the stress tensor in terms of half-sphere integrals to be evaluated with the inhomogeneous velocity distribution function of the surrounding gas, more specifically, its approximation in terms of a finite number of moments. A worked out example covers Grad's 13 moment approximation in and out of the so-called hydrodynamic approximation. We implement an accommodation coefficient characterizing the collision process in order to derive the tracer particle's complete equations of motion in a form which offers the possibility for immediate numerical implementation, and the analytical exploration of the effect of particle shape and size on phoretic drift velocity. Explicit expressions for axisymmetric, spherical, cylindrical, and also cuboidal particles are presented, discussed, and successfully compared with the rarely available, previously treated special cases, thus supporting the unifying approach presented in this manuscript. © *2006 American Institute of Physics*. [DOI: 10.1063/1.2217946]

I. INTRODUCTION

As demonstrated recently for spherical tracer (aerosol) particles, phoretic forces caused by inhomogeneities in the properties of the solvent, e.g., temperature, pressure, and velocity field, give rise to combined thermo-, baro-, and rheophoresis, respectively.[1] Thermophoretic forces caused by a temperature gradient induce dust structures, are of central interest in the scavenging of aerosol particles in clouds, when droplets and/or ice crystals grow or evaporate, during the fall of hydrometeors,[2,3] influence the velocity measurements in particle image velocimetry measurements,[4] and have been discussed in the context of nonequilibrium thermodynamics,[1,5,6] and in terms of a kinetic description,[7–10] leading to a stochastic differential equation for a tracer particle in a solvent.[1,11] In contrast to thermophoretic forces, barophoretic effects caused by pressure gradients,[12,13] and rheophoretic forces caused by velocity field gradients have been considered less frequently and not yet elaborated in an extensive, complete, or unifying fashion for nonspherical tracers.

Most aerosol particles are not spherical,[3,14–16] and it is therefore of considerable interest to examine the effect of particle shape on phoretic motion.[17,18] In this article we will present explicit expressions for the diverse phoretic forces on dissolved ellipsoidal, cylindrical, and cuboidal tracer particles derived from forces on surface elements.[1] These results will be obtained via kinetic theory in a conceptually transparent manner for particles of arbitrary convex shape, and for arbitrary solvent velocity distribution functions by half-sphere integrations over solvent velocity distribution functions before and after a collision with the tracer particle. The simultaneous incorporation of thermo-, baro-, and rheophoresis is complete in the sense that it accounts for inhomogeneities in all of the independent field variables of a nonisothermal hydrodynamic description of the solvent, but our approach equally allows to study the "nonhydrodynamic" regime. As thoroughly discussed earlier,[13,19] there is no simple way to account for inertia and diffusion within a hydrodynamic framework, and a kinetic approach is necessary. The calculations to be presented can be considered as "bruteforce" approach, less elegant (but still including) those presented earlier,[10] but involve no approximations, and may be performed, for complex shapes, with the help of a symbolic programming language.[20] Particles suspended in rarefied gases, e.g., aerosols, are often nonspherical.[3] Nevertheless, calculation of phoretic effects for nonspherical particles is scarce.[10,21] In this article, we describe the new approach, give specific results, and compare with earlier expressions and experiments.

The resulting forces and torques can be used to write down both the Langevin dynamics and the Fokker-Planck equation (FPE) for the tracer particle, suitable for immediate numerical implementation.[1] The same reference embedded the dynamics of the tracer particle into a wider description that encompasses the continuum equations for the nonisothermal hydrodynamics of the solvent. Beyond-equilibrium thermodynamics[22] had been used to examine the phoretic effects from a nonkinetic perspective. For a large class of symmetric convex bodies such as polyhedra, the phoretic forces (but not the torques) in the presence of a temperature gradient have been calculated earlier in an elegant fashion by

a)Electronic mail: mk@mat.ethz.ch
b)Electronic mail: mhuetter@mat.ethz.ch

Fernández de la Mora.[10] Due to the polyhedra's discrete "nature" the forces could be obtained without performing an integral. Surface integrals, however, enter the torques and also the forces for any continuously shaped tracer. Another special case (thin disks and cylinders) had been treated in an approximate fashion[21] where again a temperature gradient only is considered. Phoretic forces on ionic spherical particles were discussed,[23] while Ref. 24 outlines how phoretic forces could, in principle, be calculated using modified Navier-Stokes equations. Some experimental data for nonspherical (nonconvex) particle clusters subject to a temperature gradient are available.[25]

This manuscript is organized as follows. In Secs. II and III we provide background and extend the results obtained via kinetic theory[1] to include angular motion. The approach takes into account an accommodation coefficient α characterizing the collision process (elastic versus diffusive, $0 \leqslant \alpha \leqslant 1$, introduced in Ref. 26). Section III also summarizes the model ingredients, while Sec. IV reformulates phoretic forces and torques in a unifying fashion in terms of half-sphere integrals, tracer geometry-dependent integrals, and properties of the velocity distribution function of the gas. In Sec. V and Appendix A we present an analytic proof which solves the problem of evaluating half-sphere integrals of arbitrary complexity. Based on these findings, which also provide a brute-force algorithm towards the computation of phoretic accelerations for arbitrary shapes, we are in the position to formulate compact expressions for forces and torques in terms of basic surface integrals and replacement rules, cf. Sec. VI for the outline of the "procedure." Section VII presents explicit results for a distribution function expanded in Sonine tensorial polynomials, which includes Grad's 13 moment expansion in the hydrodynamic approximation as a special case. We apply the general expressions to tracer particles of various shapes in Sec. VIII and Appendix B, and offer recipes on how to generalize results to more complex situations albeit the calculations tend to become tedious beyond the (comparably high compared to previous works) level of description chosen here. Next, we show how results simplify in the isotropic phase (Sec. IX). We discuss and eventually visualize the findings, and illustrate the link between our results and experimental observations.

II. KINETIC THEORY REVISITED

The total force $\mathbf{F}$ and torque $\mathbf{T}$ acting on a convex tracer particle with surface S can be calculated as surface integrals,

$$\mathbf{F} = -\int_S \mathbf{\Pi} \cdot \mathbf{n} dS, \tag{1a}$$

$$\mathbf{T} = -\int_S \boldsymbol{r} \times \mathbf{\Pi} \cdot \mathbf{n} dS, \tag{1b}$$

where $\mathbf{r}$ stands for the surface position vector, $\mathbf{n}$ is the outward-pointing surface normal, and $\mathbf{\Pi}=\mathbf{\Pi}(\boldsymbol{r},\mathbf{n})$ the kinetic stress tensor which, for nonuniform gases, depends on the position and orientation of the surface element as shown below. If one considers two extreme scenarios, (i) ideally elastic collisions of the gas with the tracer particle and (ii) diffusive collisions which immediately restore an equilibrium velocity (Mawellian) distribution function in the body-fixed frame, one can introduce an accommodation coefficient α with $\alpha \in [0,1]$ which allows to cover these extremes and all intermediate (realistic) situations in an approximate fashion. The diffusively scattered particles obey a Maxwell velocity distribution function with vanishing average velocity with respect to the moving tracer particle. The temperature of the entire tracer particle coincides with the temperature of the undisturbed gas at its center of mass. The range of applicability of this assumption has been extensively discussed.[27] Further taking into account the uncrossability of the tracer particle it has been shown earlier[1,26] that the negative force onto a surface element, under the above mentioned assumptions, becomes[55]

$$-\mathbf{\Pi} \cdot \mathbf{n} = p[4(1-\alpha)\mathbf{nn} + 2\alpha \mathbf{1}] \cdot \mathbf{Z}_1 - \alpha p \sqrt{\pi} Z_0 \mathbf{n}, \tag{2}$$

with isotropic pressure p and unity matrix $\mathbf{1}$. The quantities Z_0 and $\mathbf{Z}_1$ denote half-space integrals over dimensionless velocities $\tilde{\mathbf{c}}$ of gas particles, i.e., particular "moments" of the dimensionless velocity distribution function f_T^* in the tracer-fixed frame,

$$\mathbf{Z}_k(\mathbf{n}) \equiv -\mathbf{n} \cdot \int_{\mathbf{n}\cdot\tilde{\mathbf{c}}<0} (\otimes^{k+1}\tilde{\mathbf{c}}) f_T^*(\tilde{\mathbf{c}}) d^3\tilde{c}, \tag{3}$$

where $(\otimes^n \tilde{\mathbf{c}})$ denotes the n-fold tensor product of $\tilde{\mathbf{c}}=\sqrt{\beta}\mathbf{c}$ with $\beta \equiv m_s/(2k_BT)$, mass m_s of a gas particle, peculiar velocity of the gas particle $\mathbf{c}$, temperature T at location $\mathbf{r}$ of the nonuniform, tracer-free gas, and $\int f_T^*(\tilde{\mathbf{c}}) d^3\tilde{c}=1$ defines the coefficient of proportionality between nondimensional f_T^* and dimensional f_T velocity distribution functions which is usually normalized as $\int f_T(\mathbf{c}) d^3c = n_s$ with n_s the particle number density of gas particles.

We further mention that the distribution function of gas particles just after colliding with the tracer particle at its surface normal $\mathbf{n}$ is known as soon as Z_0 and $\mathbf{Z}_1$ were calculated.[1,26]

III. MODEL INGREDIENTS

In order to evaluate the above formulas, we need to specify the model, i.e., (A) a velocity distribution function characterized through so called $\boldsymbol{\alpha}$ tensors described below and (B) a shape of the tracer particle characterized through a surface $\boldsymbol{r}(v_1,v_2)$ parametrized by v_1 and v_2.

(A) Velocity distribution function and its $\boldsymbol{\alpha}$ tensors. Any nonuniform distribution function of the tracer free gas $f(\mathbf{c})$ or equally $f^*(\tilde{\mathbf{c}})$ can be expanded into tensorial associated Laguerre (Sonine) polynomials and thus

$$f_T^*(\tilde{\mathbf{c}}) = f^*(\tilde{\mathbf{c}} + \tilde{\mathbf{c}}_T + \Delta\tilde{\boldsymbol{\omega}}_T \times \boldsymbol{r}) \tag{4}$$

can be parameterized by tensorial coefficients $\boldsymbol{\alpha} = \boldsymbol{\alpha}(\tilde{\mathbf{c}}_T, \Delta\tilde{\boldsymbol{\omega}}_T)$ which are constants with respect to $\tilde{\mathbf{c}}$, but depend on the peculiar velocity $\tilde{\mathbf{c}}_T$ and peculiar angular velocity $\boldsymbol{\Delta}\tilde{\omega}_T$ of the tracer particle (both quantities again reduced by $\sqrt{\beta}$). The $\boldsymbol{\alpha}$ tensors are defined from the distribution function $f^*(\tilde{\mathbf{c}})$ of the undisturbed gas through the representation

$$f_T^*(\tilde{\mathbf{c}}) = \pi^{-3/2} e^{-\tilde{c}^2} \sum_{m=0}^{M} \sum_{i=0}^{\infty} \sum_{n=0}^{1} \tilde{c}^{2i} \boldsymbol{\alpha}_{m,i}^{n} \odot^{m+n} (\otimes^n \mathbf{r})(\otimes^m \tilde{\mathbf{c}}). \quad (5)$$

How to explicitly read off the $\boldsymbol{\alpha}$'s from any given (approximate) solution of the Boltzmann equation $f(\mathbf{c})$ in the absence of tracer particles is worked out in detail in Appendix C. All information about the distribution function to be used in (3) is thus contained in $\boldsymbol{\alpha}$ and any possible distribution function is uniquely specified through its $\boldsymbol{\alpha}_{m,n}^0(\tilde{\mathbf{c}}_T)$ coefficients because of the relationship

$$\boldsymbol{\alpha}_{m,i}^1 \cdot \boldsymbol{r} = (\Delta \tilde{\boldsymbol{\omega}}_T \times \boldsymbol{r}) \cdot (\boldsymbol{\nabla}_{\mathbf{c}_T} \boldsymbol{\alpha}_{m,n}^0), \quad (6)$$

which follows from (4) and (5) alone if we neglect quadratic and higher order terms in $\tilde{\mathbf{c}}_T$ for the reason that the tracer particle can be assumed to be heavy and thus slow compared with a representative gas particle.[1] In (5) the symbol $\odot^n$ stands for an n-fold contraction. For example, if $f^*(\tilde{\mathbf{c}}) = \pi^{-3/2} \exp(-\tilde{c}^2)$ is the nondimensional equilibrium Maxwell distribution, the reader should convince her-or himself that $\alpha_{0,0}^0 = 1$ and $\boldsymbol{\alpha}_{1,0}^0 = -2\tilde{\mathbf{c}}_T$. From (6) then follows $\boldsymbol{\alpha}_{1,0}^1 = -2\boldsymbol{\Delta}\tilde{\omega}_T \times \mathbf{r}$ and all other $\boldsymbol{\alpha}$ coefficients vanish. Due to the relationship (6) it is obvious, that one can consider $\Delta\tilde{\boldsymbol{\omega}}_T = 0$ and (5) with $n=0$ to derive all $\boldsymbol{\alpha}$ tensors for given $f^*(\tilde{\mathbf{c}})$. The remainder of this manuscript we will present worked out examples.

As we will see, starting from a non-Maxwellian, nonuniform distribution function leads to phoretic motion where the peculiar translational and rotational velocities are nonzero and the tracer particle drifts in "direction" of moments (usually temperature, pressure, flow, or other field gradients) of the distribution function. The exact form of the forces and torques will depend on the shape and orientation of the tracer particle. It is essential to note that the velocity distribution function of the carrier gas is not disturbed by the presence of the tracer particle, which is a reasonable assumption for large Knudsen numbers also adopted by others.[26,28]

(B) Geometry of tracer particle. To perform the surface integral in (1) we need to define the convex geometry of the tracer particle. For a convex body, all points on the line connecting two arbitrary points on its surface must be located inside its body. Limiting the study to convex particles has important ramifications for the following calculation. Namely, solvent particles which have collided with the tracer particle will experience subsequent collisions in the surrounding gas. A more technical aspect is the fact that the directions available for incoming and scattered particles is a half sphere, which amounts to the calculations of the so-called half-sphere integrals ubiquitous below. Any surface of a convex tracer is defined by a position vector $\mathbf{r} = \mathbf{r}(v_1, v_2)$ parametrized by two variables v_1 and v_2, and their ranges ∂_1 and ∂_2. The surface normal $\mathbf{n}$ is then obtained from the surface vector $\mathbf{s} \equiv (\partial \mathbf{r}/\partial v_1) \times (\partial \mathbf{r}/\partial v_2)$ by normalization, $\mathbf{n} = \mathbf{s}/s$, $s = |\mathbf{s}|$, and one has to choose $v_{1,2}$ in an order such that $\mathbf{n}$ points outward the convex tracer particle, cf. Table III.

IV. REFORMULATION IN TERMS OF GEOMETRY-DEPENDENT INTEGRALS

Once the task has been stated through Eqs. (1)–(3), supplemented by $f_T^*(\mathbf{c})$, i.e., $\boldsymbol{\alpha}$ tensors, and a geometry $\mathbf{r}(v_1, v_2)$ of the tracer particle, we rewrite it in a form which separates contributions which can be calculated analytically, and others, which require a remaining purely geometry-dependent integral (to be denoted as $\boldsymbol{G}$ below).

Introducing the abbreviation $\boldsymbol{Y}$ for a specific parametrized integral over the tracer particle's surface,

$$\boldsymbol{Y}_k^{x,y,z} \equiv \int p \mathbf{Z}_k \odot^x (\otimes^y \mathbf{n})(\otimes^z \mathbf{r}) dS, \quad (7)$$

where the pressure p is under the integral and to be evaluated at the tracer particle surface, we can rewrite (1), i.e, forces $\mathbf{F}$ and torques $\mathbf{T}$, as follows:

$$\mathbf{F} = \boldsymbol{A}^{(0)}, \quad (8a)$$

$$\mathbf{T} = \boldsymbol{\epsilon} : \boldsymbol{A}^{(1)}, \quad (8b)$$

with totally antisymmetric (Levi-Cività) tensor $\boldsymbol{\epsilon}$ of rank 3 and

$$\boldsymbol{A}^{(\mathbf{z})} \equiv \frac{2(1-\alpha)}{\sqrt{\pi}} \boldsymbol{Y}_1^{1,2,z} + \frac{\alpha}{\sqrt{\pi}} \boldsymbol{Y}_1^{0,0,z} - \frac{\alpha}{2} \boldsymbol{Y}_0^{0,1,z}. \quad (9)$$

Making use of (i) the half-unit-sphere integrals (tensors $\boldsymbol{\Omega}_m$ of rank $m \geq 0$) defined as

$$\boldsymbol{\Omega}_m(\mathbf{n}) \equiv -\frac{1}{\pi} \int_{\hat{\mathbf{c}} \cdot \mathbf{n} < 0} (\otimes^m \hat{\mathbf{c}})(\mathbf{n} \cdot \hat{\mathbf{c}}) d^2 \hat{c}, \quad (10)$$

and evaluated analytically in Appendix A, (ii) the known Gaussian integral

$$2\int_0^\infty e^{-\tilde{c}^2} \tilde{c}^n d\tilde{c} = \Gamma[(n+1)/2] \equiv [(n-1)/2]!,$$

involving the gamma function Γ, and (iii) defining purely geometry-dependent integrals $\boldsymbol{G}$ ($\boldsymbol{G}_{m,n}^{x,y,z}$ is a tensor of rank $n + m + y + z - 2x$) as

$$\boldsymbol{G}_{m,n}^{x,y,z} \equiv \int (\otimes^n \mathbf{r}) \boldsymbol{\Omega}_m \odot^x (\otimes^y \mathbf{n})(\otimes^z \mathbf{r}) dS, \quad (11)$$

we can express $\boldsymbol{Y}$ and thus $\boldsymbol{A}$ and the forces and torques purely in terms of (given) model parameters $\boldsymbol{\alpha}$ and (remaining) geometry-dependent integrals $\boldsymbol{G}$, since we now have, more explicitly,

$$\boldsymbol{Y}_k^{x,y,z} = \sum_{n,m,i} \left(1 + i + \frac{m+k}{2}\right)! \boldsymbol{\alpha}_{m,i}^n \odot^{n+m} [p_0 \boldsymbol{G}_{m+k,n}^{x,y,z} + (\tilde{\boldsymbol{\nabla}} p) \cdot \boldsymbol{G}_{m+k,n+1}^{x,y,z}], \quad (12)$$

with

$$\tilde{\nabla} p = \begin{cases} \dfrac{1}{\sqrt{\beta}} \nabla (\sqrt{\beta} p) = \nabla p - \dfrac{1}{2} p_0 \nabla \ln T & \text{if multiplied with } \tilde{\mathbf{c}}_T \text{ or } \Delta\tilde{\boldsymbol{\omega}}_T, \\ \nabla p & \text{otherwise.} \end{cases} \tag{13}$$

We hereby also demonstrated how to incorporate pressure gradients into the formalism, albeit the dominating contribution to the force proportional in the pressure gradient will not involve a surface integral as will be seen below. In the expression for $\boldsymbol{Y}_k^{x,y,z}$, higher than first order spatial derivatives are neglected. The triple sum over m, n, and i usually reduces to a summation over very few terms, as we will see below, and also k, z, and n can take only values 0 or 1, further $x \leqslant k$, $y \leqslant 2$, and the ranges for m and i depend on the chosen model. Grad's 13 moment approximation for example is covered by $M=3$, $m \leqslant 3$, and $i \leqslant 1$. The notation (13) arises because we had introduced—and now take care of—the velocity $\tilde{\mathbf{c}}_T$ which we made dimensionless by using $\sqrt{\beta} \propto 1/\sqrt{T}$ which is not a constant on the tracer's surface in the presence of a temperature gradient. Technically, (13) means that we can perform all calculations using $\tilde{\boldsymbol{\nabla}} p = \boldsymbol{\nabla} p$ and have to replace in the final results for forces and torques any occurrence of a (scalar or tensorial) product $\tilde{\mathbf{c}}_T \boldsymbol{\nabla} p$ by $\mathbf{c}_T \boldsymbol{\nabla}(\sqrt{\beta} p)$, or equivalently, $\tilde{\mathbf{c}}_T \boldsymbol{\nabla} p$ by $\tilde{\mathbf{c}}_T(\boldsymbol{\nabla} p - (p_0/2)\boldsymbol{\nabla} \ln T)$ (similarly for $\Delta\tilde{\boldsymbol{\omega}}_T$). As we will see below, this operation usually is relevant just for a single term with $m=1$, $i=n=0$. To summarize, forces and torques can be calculated in a "brute-force" fashion through calculating the geometric $\boldsymbol{G}$ tensors. These tensors, in turn, are simple sums of base-surface integrals to be introduced below for which analytic expressions will be often available.

V. HALF-SPHERE INTEGRALS

In order to evaluate the $\boldsymbol{G}$ tensors we need (i) the geometryies of the tracer particle, $\boldsymbol{r}(v_1, v_2)$ and $\boldsymbol{n}(v_1, v_2)$, in terms of surface parameters $v_{1,2}$ (including their support) and (ii) to know how to evaluate the geometry-independent $\boldsymbol{\Omega}$'s in terms of $\mathbf{n}$. Concerning (i) we are free to choose a geometry but analytic results were not available for arbitrary ones. We will hence choose, for illustrative purposes, spherical, cylindrical, ellipsoidal, and cuboidal tracer particles for which $\boldsymbol{G}$ tensors can be calculated, in principle, manually. Complex geometries can be handled through a program[20] which implements the strategy outline here. (ii) As shown in Appendix A the $\boldsymbol{\Omega}_k$ tensors are linear combinations of mixed, symmetric tensors of the kind $[(\otimes^m \mathbf{1})(\otimes^{n-2m}\mathbf{n})]_{\text{sym}}$, where $[\cdots]_{\text{sym}}$ denotes the dyadic produced by the dots, made symmetric in all indices, and subsequently normalized. For example, $[(\otimes^2 \mathbf{e}_1)(\otimes^1 \mathbf{n})]_{\text{sym}} = (\mathbf{e}_1\mathbf{e}_1\mathbf{n} + \mathbf{e}_1\mathbf{n}\mathbf{e}_1 + \mathbf{n}\mathbf{e}_1\mathbf{e}_1)/3$. The analytical result reads

$$\boldsymbol{\Omega}_m = \sum_{p=0}^{\text{int}(m/2)} c_m^p [(\otimes^p \mathbf{1})(\otimes^{m-2p}\mathbf{n})]_{\text{sym}}, \tag{14}$$

for arbitrary integers $m \geqslant 0$, with coefficients

$$c_m^p \equiv \frac{m!}{\sqrt{\pi}(1+(m/2))!p!}(-1)^{m-p} \times \sum_{q=0}^{\text{int}(m/2)} \frac{(-1)^q q! \left(q-\frac{1}{2}\right)!((m/2)-q)!}{(q-p)!(2q)!(m-2q)!}, \tag{15}$$

where $\text{int}(m/2)=m/2$ and $\text{int}(m/2)=(m-1)/2$ for even and odd m, respectively. $\boldsymbol{\Omega}$ tensors of arbitrary rank are thus available using basic combinatorial rules,[20] some relevant contraction rules are worked out in Tables I and II. Sample values for coefficients and tensors are $c_0^0=1$, $c_1^0=-2/3$, $c_2^0=1/4$, $c_2^1=1/4$, $c_3^0=0$, $c_3^1=-2/5$, and $\Omega_0=1$, $\boldsymbol{\Omega}_1=-\frac{2}{3}\mathbf{n}$, and $\boldsymbol{\Omega}_2=\frac{1}{4}(\mathbf{n}\mathbf{n}+\mathbf{1})$, respectively. The $\boldsymbol{G}$ tensors (11) are then evaluated by replacing $\int dS$ by the double integral $\int_{\partial_1} dv_1 \int_{\partial_2} dv_2 s$ with s defined in Sec. III B. Sections IV and V suffice to set up a code to compute results numerically, or symbolically, but does not provide any insight about tensorial symmetries affecting the physical mechanism.

VI. COMPACT NOTATION FOR GIVEN LEVEL OF DESCRIPTION

The strategy presented in the foregoing section leads us directly to generalize the compact notation proposed in Ref. 10 and 21. Instead of directly evaluating $\boldsymbol{G}$ for a chosen application, we can use contraction rules for the half-sphere integrals (summarized in Table I) still within the integrand to

TABLE I. Evaluated expressions for the tensors $[(\otimes^p\mathbf{1})(\otimes^{m-2p}\mathbf{n})]_{\text{sym}} \odot^x (\otimes^y \mathbf{n})$ of rank $m-2x+y$, which appear in connection with the $\boldsymbol{G}$ tensors (11). The integers m, p, x, and y are subject to constraints: $m \geqslant 0$, $0 \leqslant p \leqslant m/2$, $0 \leqslant x \leqslant m$, and $x \leqslant y$. A Maxwell distributions involves $m \leqslant 2$, Grad's 13 moment expansion needs $m \leqslant 4$, i.e., $m \leqslant \max \text{rank}(\boldsymbol{\alpha})+1$ in general. The $\mu\nu\kappa$ component of the $(\mathbf{ini})$ and $(\mathbf{1n})$ tensors read $\delta_{\mu\kappa}n_\nu$ and $\delta_{\mu\nu}n_\kappa$, respectively; $(\otimes^0\mathbf{n})=1$, $(\otimes^1\mathbf{n})=\mathbf{n}$, $(\otimes^2\mathbf{n})=\mathbf{nn}$, etc: the bold $\mathbf{1}$ symbol denotes the unity matrix.

m	p	x	$[(\otimes^p\mathbf{1})(\otimes^{m-2p}\mathbf{n})]_{\text{sym}} \odot^x (\otimes^y\mathbf{n})$
m	0	$\geqslant 0$	$(\otimes^{m-2x+y}\mathbf{n})$
2	1	0	$\mathbf{1}(\otimes^y\mathbf{n})$
		$\geqslant 1$	$(\otimes^{2-2x+y}\mathbf{n})$
3	1	0	$\frac{1}{3}[\mathbf{1}(\otimes^{y+1}\mathbf{n})+\mathbf{ini}(\otimes^y\mathbf{n})+\mathbf{n1}(\otimes^y\mathbf{n})]$
		1	$\frac{1}{3}[\mathbf{1}(\otimes^{y-1}\mathbf{n})+2(\otimes^{y+1}\mathbf{n})]$
		$\geqslant 2$	$(\otimes^{3-2x+y}\mathbf{n})$
4	1	0	$[\mathbf{1nn}]_{\text{sym}}(\otimes^y\mathbf{n})$
		1	$\frac{1}{6}[\mathbf{1}(\otimes^y\mathbf{n})+\mathbf{ini}(\otimes^{y-1}\mathbf{n})+3(\otimes^{y+2}\mathbf{n})+\mathbf{n1}(\otimes^{y-1}\mathbf{n})]$
		2	$\frac{1}{6}[\mathbf{1}(\otimes^{y-2}\mathbf{n})+5(\otimes^y\mathbf{n})]$
		$\geqslant 3$	$(\otimes^{4-2x+y}\mathbf{n})$
4	2	0	$[\mathbf{11}]_{\text{sym}}(\otimes^y\mathbf{n})$
		1	$\frac{1}{3}[\mathbf{1}(\otimes^y\mathbf{n})+\mathbf{ini}(\otimes^{y-1}\mathbf{n})+\mathbf{n1}(\otimes^{y-1}\mathbf{n})]$
		2	$\frac{1}{3}[\mathbf{1}(\otimes^{y-2}\mathbf{n})+2(\otimes^y\mathbf{n})]$
		$\geqslant 3$	$(\otimes^{4-2x+y}\mathbf{n})$

TABLE II. Evaluated expressions for the tensors $\mathbf{\Omega}_m \odot^x (\otimes^y \mathbf{n}) = \Sigma_{p=0}^{\text{int}(m/2)} c_m^p [(\otimes^p \mathbf{1})(\otimes^{m-2p}\mathbf{n})]_{\text{sym}} \odot^x (\otimes^y \mathbf{n})$ of rank $m-2x+y$, with the coefficients c_m^p given in (15). We make use of the results collected in Table I. These tensors simplify the analysis of the $\boldsymbol{G}$ tensors (11) without actually evaluating an integral. The integers m, x, and y are subject to constraints: $m \geqslant 0$, $0 \leqslant x \leqslant m$, and $x \leqslant y$. A Maxwell distributions involves $m \leqslant 2$, Grad's 13 moment expansion needs $m \leqslant 4$, i.e., $m \leqslant \max \text{rank}(\boldsymbol{\alpha})+1$ in general.

m	x	$\mathbf{\Omega}_m \odot^x (\otimes^y \mathbf{n})$
0	0	$(\otimes^y \mathbf{n})$
1	$\geqslant 0$	$-\frac{2}{3}(\otimes^{y+1-2x}\mathbf{n})$
2	0	$\frac{1}{4}[(\otimes^{y+2}\mathbf{n})+\mathbf{1}(\otimes^y \mathbf{n})]$
2	$\geqslant 1$	$\frac{1}{2}(\otimes^{y+2-2x}\mathbf{n})$
3	0	$-\frac{2}{5}[\mathbf{1n}]_{\text{sym}}(\otimes^y \mathbf{n})$
3	1	$-\frac{2}{15}[\mathbf{1}(\otimes^{y-1}\mathbf{n})+2(\otimes^{y+1}\mathbf{n})]$
3	$\geqslant 2$	$-\frac{2}{5}(\otimes^{y+3-2x}\mathbf{n})$
4	0	$-\frac{1}{24}(\otimes^{y+4}\mathbf{n})+\frac{1}{4}[\mathbf{1nn}]_{\text{sym}}(\otimes^y \mathbf{n})+\frac{1}{8}[\mathbf{11}]_{\text{sym}}(\otimes^y \mathbf{n})$
4	1	$\frac{1}{4}[\mathbf{1n}]_{\text{sym}}(\otimes^{y-1}\mathbf{n})+\frac{1}{12}(\otimes^{y+2}\mathbf{n})$
4	2	$\frac{1}{12}[\mathbf{1}(\otimes^{y-2}\mathbf{n})+3(\otimes^y \mathbf{n})]$
4	$\geqslant 3$	$\frac{1}{3}(\otimes^{y+4-2x}\mathbf{n})$

simplify $\boldsymbol{G}$ and thus obtain compact expressions for forces and torques in terms of more basic surface integrals. Such an approach is possible if we had specified the distribution function of the surrounding gas, however, it is already sufficient having specified the range of indices m,i of nonvanishing $\boldsymbol{\alpha}_{m,i}^0$ tensors for the problem at hand, cf. Sec. VIII and Table II. Let us therefore discuss the compact notation before turning to an explicit representation for a distribution function of the gas.

In order to outline our procedure—based on Secs. IV and V—which allows to write down compact results for forces and torques in terms of a few basic surface integrals for even the most complex situations (arbitrary $\boldsymbol{\alpha}'s$), it is completely sufficient to consider a Maxwellian distribution in the absence of angular motion only,

$$f^*(\tilde{\mathbf{c}}) = \pi^{-3/2} e^{-(\tilde{\mathbf{c}}+\tilde{\mathbf{c}}_T)^2}, \tag{16}$$

which is, for $c_T \ll c$ of the form (5) with $\alpha_{0,0}^0 = 1$ and $\boldsymbol{\alpha}_{1,0}^0 = -2\tilde{\mathbf{c}}_T$ leading to force contributions to be denoted as $\mathbf{F}[0]$ and $\mathbf{F}[0,\tilde{\mathbf{c}}_T]$ (related to zeroth moment), respectively. Inserting these coefficients into (8) and (9) with (11) and (12), and $\mathbf{\Omega}_{0,1,2}$ from Sec. V directly produces the following "compact" form for the total force $\mathbf{F}=\mathbf{F}[0]+\mathbf{F}[0,\tilde{\mathbf{c}}_T]+\mathbf{F}[0,\Delta\tilde{\boldsymbol{\omega}}_T]$ and torque $\mathbf{T}=\mathbf{T}[0]+\mathbf{T}[0,\tilde{\mathbf{c}}_T]+\mathbf{T}[0,\Delta\tilde{\boldsymbol{\omega}}_T]$ exerted by the uniform gas,

$$\mathbf{F}[0] = -pA\langle \mathbf{n}\rangle_S, \tag{17a}$$

$$\mathbf{F}[0,\tilde{\mathbf{c}}_T] = -\frac{4pA}{\sqrt{\pi}}\tilde{\mathbf{c}}_T \cdot \left[\frac{\alpha}{4}\langle \mathbf{1}\rangle_S + \left(1-\frac{3}{4}\alpha+\frac{\pi}{8}\alpha\right)\langle \mathbf{nn}\rangle_S\right], \tag{17b}$$

where we use (througout this paper) the definitions

$$\langle \boldsymbol{B}\rangle_S \equiv \frac{1}{A}\int \boldsymbol{B}\,dS, \tag{18a}$$

$$A \equiv \int dS. \tag{18b}$$

Here S stands for the geometry of the tracer, we will use symbols according to Table III when evaluating surface integrals. It essentially follows from (12) that the remaining force $\mathbf{F}[0,\Delta\tilde{\boldsymbol{\omega}}_T]$ and all torque contributions do not require, concerning their compact notation (17), any additional calculation. This is so because we keep all averages $\langle\cdots\rangle_S$ (surface integrals) unevaluated which is an integral part of our procedure at this stage; even those averages which seem to vanish for obvious reasons. In particular, we must write $\langle \mathbf{1}\rangle_S$ rather than $\mathbf{1}$, and we must keep $\langle \mathbf{n}\rangle_S$ rather than removing this term. This procedure ensures that we can use the following replacement rules, which hold not only for this particular simple example, but are valid also in the most general cases (including the more general case which follows in Sec. VII),

$$\mathbf{F}[\bullet,\Delta\tilde{\boldsymbol{\omega}}_T] = \mathbf{F}[\bullet,\tilde{\mathbf{c}}_T] \quad \text{upon replacing} \quad \tilde{\mathbf{c}}_T \odot \langle \boldsymbol{B}\rangle_S \to \Delta\tilde{\boldsymbol{\omega}}_T \times \langle \mathbf{r}\odot \boldsymbol{B}\rangle_S, \tag{19}$$

$$\mathbf{T}[\bullet] = \boldsymbol{\epsilon}:(\mathbf{F}[\bullet]) \quad \text{upon replacing } \langle \boldsymbol{B}\rangle_S \to \langle \boldsymbol{B}\mathbf{r}\rangle_S, \tag{20}$$

where $\bullet$, $\odot$, and $\boldsymbol{B}$ are placeholders for arbitrary arguments, contractions, and integrands, respectively, the cross product ($\times$) in (19) has priority against a tensorial ($\odot$) product, and even the bracket around $\mathbf{F}[\bullet]$ in (20) is important since it indicates that contraction inside $\mathbf{F}[\bullet]$ are performed before

TABLE III. Surface vector $\mathbf{r}$ scanning the surface, surface normal $\mathbf{n}=\mathbf{s}/s$ with $\mathbf{s}\equiv(\partial\mathbf{r}/\partial v_1)\times(\partial\mathbf{r}/\partial v_2)$, and $s=|\mathbf{s}|$ for various gometries: sphere of radius R, uniaxial ellipsoid with radius R and axis ratio Q, cyclindrical tube of radius R and height to diameter ratio $Q_\parallel$, the two flat end caps ($\pm$) for the same cylinder, faces $\mu\nu\kappa \in \{123,132,213,231,312,321\}$ of a cuboid with edge lengths $L_{1,2,3}$, of a cube with edge length L, and of an axialsymmetric particle aligned in $\mathbf{e}_3$ direction, characterized by a function $\rho(v_2)$ [it has no open ends if $\rho(\pm 1)=0$ and includes the uniaxial ellipsoid as a special case]. The base vectors $\mathbf{e}_{1,2,3}$ define the coordinate system in which forces and torques are also expressed. We introduced the abbreviation $\mathbf{e}^{\pm iv_1} \equiv \cos v_1 \mathbf{e}_1 \pm \sin v_1 \mathbf{e}_2$.

Geometry symbol	$\mathbf{r}$	$\mathbf{n}=\mathbf{s}/s$	$s=\|\mathbf{s}\|$	$v_1 \in$	$v_2 \in$
Sphere ○	$R[\mathbf{e}^{iv_1}\sqrt{1-v_2^2}+v_2\mathbf{e}_3]$	$\mathbf{r}/R$	R^2	$[0,2\pi]$	$[-1,1]$
Cylindrical tube ‖	$R[\mathbf{e}^{iv_1}+Q_\parallel v_2\mathbf{e}_3]$	$\mathbf{e}^{iv_1}$	R	$[0,2\pi]$	$[-1,1]$
Flat end caps ∩	$\pm R[\mathbf{e}^{\pm iv_1}+Q_\parallel \mathbf{e}_3]$	$\pm\mathbf{e}_3$	$R^2\|v_2\|$,	$[0,2\pi]$	$[0,1]$
Cuboid □	$\frac{1}{2}\epsilon_{\mu\nu\kappa}(L_\mu\mathbf{e}_\mu+v_1L_\nu\mathbf{e}_\nu+v_2L_\kappa\mathbf{e}_\kappa)$	$\epsilon_{\mu\nu\kappa}\mathbf{e}_\mu$	$\frac{1}{2}L_\nu L_\kappa$	$[-1,1]$	$[-1,1]$
Cube □	$\frac{1}{2}\epsilon_{\mu\nu\kappa}L(\mathbf{e}_\mu+v_1\mathbf{e}_\nu+v_2\mathbf{e}_\kappa)$	$\epsilon_{\mu\nu\kappa}\mathbf{e}_\mu$	$\frac{1}{2}L^2$	$[-1,1]$	$[-1,1]$
Axisymmetric ⊖	$\rho(v_2)[\mathbf{e}^{iv_1}]+Qv_2\mathbf{e}_3$	$s^{-1}\rho(Q\mathbf{e}^{iv_2}-\rho'\mathbf{e}_3)$	$\rho\sqrt{Q^2+\rho'^2}$	$[0,2\pi]$	$[-1,1]$

the double contraction with $\boldsymbol{\epsilon}$. These rules are easily proven using the expressions of Sec. IV. They particularly reflect the way we eliminate the $\boldsymbol{\alpha}^1_{m,i}$ tensors via (6). To illustrate these rules let us give two examples. (i) We have $\mathbf{T}[0]=\boldsymbol{\epsilon}:\mathbf{F}[0]$ still subject to replacements (20), and therefore, using (17a), $\mathbf{T}[0]=-pA\boldsymbol{\epsilon}:\langle\mathbf{nr}\rangle_S$ which vanishes for a sphere where $\langle\mathbf{nr}\rangle_S$ is symmetric. (ii) Using the replacement rules (19) and (20), the torque $\mathbf{T}[0,\Delta\tilde{\boldsymbol{\omega}}_T]$ can be related to the expression for the friction force $\mathbf{F}[0,\tilde{\mathbf{c}}_T]$. In particular for a sphere, it follows from (17b) that the relation $\mathbf{F}[0,\tilde{\mathbf{c}}_T]\propto\tilde{\mathbf{c}}_T$ brings about the torque relation $\mathbf{T}[0,\Delta\tilde{\boldsymbol{\omega}}_T]\propto\Delta\tilde{\boldsymbol{\omega}}_T$.

Replacement rules similar to (19) and (20) have been employed by Rohatschek and Zulehner[29] for a carrier gas described by the (equilibrium) Maxwellian velocity distribution. Extension to situations where the carrier gas is out of equilibrium (e.g., Grad's 13 moment expansion) requires the extended description presented in Sec. IV. Only then it becomes clear to which specific terms and shape dependent surface integrals the rules (19) and (20) have to be applied. Next, the applicability of the scheme is extended by generalizing (17).

VII. COMPACT RESULTS FOR GRAD'S 13 MOMENT EXPANSION

As an important special case of the above results, we can write down compact results for the case where the nonuniform gas is fully characterized by its first two tensorial moments, known as Grad's 13 moment expansion (Appendix C covers more general cases). Here, the velocity distribution function of the carrier gas, unperturbed by the tracer particle, reads[1,22,30]

$$f^*(\tilde{\mathbf{c}}) = \pi^{-3/2}e^{-\tilde{c}^2}[1+\langle\boldsymbol{\phi}^1_1\rangle\cdot\boldsymbol{\phi}^1_1+\langle\boldsymbol{\phi}^2_0\rangle:\boldsymbol{\phi}^2_0], \tag{21}$$

with the nth rank tensorial, orthonormal coefficients $\boldsymbol{\phi}^n_k(\tilde{\mathbf{c}})$, in particular,

$$\boldsymbol{\phi}^1_1 = \frac{2}{\sqrt{5}}\left(\frac{5}{2}-\tilde{c}^2\right)\tilde{\mathbf{c}}, \tag{22a}$$

$$\boldsymbol{\phi}^2_0 = \sqrt{2}\,\overline{\otimes^2\tilde{\mathbf{c}}} = \sqrt{2}\left(\tilde{\mathbf{c}}\tilde{\mathbf{c}}-\frac{\tilde{c}^2}{3}\mathbf{1}\right), \tag{22b}$$

and corresponding moments $\langle\boldsymbol{\phi}^n_k\rangle$ of the distribution function as explained in detail in Appendix C. By comparing $f^*(\tilde{\mathbf{c}}+\tilde{\mathbf{c}}_T)$ from (21) with (4) and (5) and assuming $\tilde{c}_T\ll\tilde{c}$ (see also Appendix C) we see that $M=3$ and the dimensionless $\boldsymbol{\alpha}$ tensors read[1] $\boldsymbol{\alpha}^0_{0,0}=1-\sqrt{5}\langle\boldsymbol{\phi}^1_1\rangle\cdot\tilde{\mathbf{c}}_T$, $\boldsymbol{\alpha}^0_{0,1}=\frac{2}{\sqrt{5}}\langle\boldsymbol{\phi}^1_1\rangle\cdot\tilde{\mathbf{c}}_T$, $\boldsymbol{\alpha}^0_{1,0}=-2\tilde{\mathbf{c}}_T-\sqrt{5}\langle\boldsymbol{\phi}^1_1\rangle+2^{3/2}\langle\boldsymbol{\phi}^2_0\rangle\cdot\tilde{\mathbf{c}}_T$, $\boldsymbol{\alpha}^0_{1,1}=\frac{2}{\sqrt{5}}\langle\boldsymbol{\phi}^1_1\rangle$, $\boldsymbol{\alpha}^0_{2,0}=\sqrt{2}\langle\boldsymbol{\phi}^2_0\rangle+\frac{14}{\sqrt{5}}\langle\boldsymbol{\phi}^1_1\rangle\tilde{\mathbf{c}}_T$, $\boldsymbol{\alpha}^0_{2,1}=-\frac{4}{\sqrt{5}}\langle\boldsymbol{\phi}^1_1\rangle\tilde{\mathbf{c}}_T$, and $\boldsymbol{\alpha}^0_{3,0}=-2^{3/2}\langle\boldsymbol{\phi}^2_0\rangle\tilde{\mathbf{c}}_T$. Corresponding $\boldsymbol{\alpha}^1$ tensors are given by (6). Using these tensors along the lines indicated in the foregoing section the complete listing of all (twelve) distinct compact contributions to the total force and an equal number of contributions to the total torque on a convex tracer particle immersed in the nonuniform gas read, with accommodation coefficient α,

$$\mathbf{F}[0] = -pA\langle\mathbf{n}\rangle_S, \tag{23a}$$

$$\mathbf{F}[\langle\boldsymbol{\phi}^1_1\rangle] = \frac{pA}{2\sqrt{5}\sqrt{\pi}}\langle\boldsymbol{\phi}^1_1\rangle\cdot[\alpha\langle\mathbf{1}\rangle_S+(4-3\alpha)\langle\mathbf{nn}\rangle_S], \tag{23b}$$

$$\mathbf{F}[\langle\boldsymbol{\phi}^2_0\rangle] = \sqrt{2}pA\langle\boldsymbol{\phi}^2_0\rangle\odot^2\Big[\left(\tfrac{3}{4}\alpha-1\right)\langle\mathbf{nnn}\rangle_S - \tfrac{3}{4}\alpha\langle[\mathbf{1n}]_{\mathrm{sym}}\rangle_S\Big], \tag{23c}$$

$$\mathbf{F}[\tilde{\boldsymbol{\nabla}}p] = -A(\boldsymbol{\nabla}p)\cdot\langle\mathbf{rn}\rangle_S, \tag{23d}$$

$$\mathbf{F}[0,\tilde{\mathbf{c}}_T] = -\frac{4pA}{\sqrt{\pi}}\tilde{\mathbf{c}}_T\cdot\left[\frac{\alpha}{4}\langle\mathbf{1}\rangle_S+\left(1-\frac{3}{4}\alpha+\frac{\pi}{8}\alpha\right)\langle\mathbf{nn}\rangle_S\right], \tag{23e}$$

$$\mathbf{F}[\langle\boldsymbol{\phi}^1_1\rangle,\tilde{\mathbf{c}}_T] = -\frac{\alpha}{2}\frac{pA}{\sqrt{5}}\{\langle\boldsymbol{\phi}^1_1\rangle\cdot(\tilde{\mathbf{c}}_T\cdot\langle\mathbf{nnn}\rangle_S)\}, \tag{23f}$$

$$\begin{aligned}\mathbf{F}[\langle\boldsymbol{\phi}^2_0\rangle,\tilde{\mathbf{c}}_T] = \frac{2^{3/2}pA}{\sqrt{\pi}}\Bigg\{&(\langle\boldsymbol{\phi}^2_0\rangle\cdot\tilde{\mathbf{c}}_T)\cdot\left[\frac{\alpha}{2}\langle\mathbf{1}\rangle_S+\left(2-\frac{3}{2}\alpha+\frac{\pi}{4}\alpha\right)\langle\mathbf{nn}\rangle_S\right]\\ &-(\langle\boldsymbol{\phi}^2_0\rangle\tilde{\mathbf{c}}_T)\odot^3\Bigg[\left(1-\frac{5}{4}\alpha\right)\langle\mathbf{nnnn}\rangle_S+3\left(1-\alpha+\frac{\pi}{8}\alpha\right)\langle[\mathbf{1n}]_{\mathrm{sym}}\mathbf{n}\rangle_S\\ &+\frac{3}{2}\alpha\langle[\mathbf{1nn}]_{\mathrm{sym}}\rangle_S+\frac{3}{4}\alpha\langle[\mathbf{11}]_{\mathrm{sym}}\rangle_S\Bigg]\Bigg\},\end{aligned} \tag{23g}$$

$$\mathbf{F}[\tilde{\boldsymbol{\nabla}}p,\tilde{\mathbf{c}}_T] = -2A\tilde{\mathbf{c}}_T\cdot\left[\frac{2}{\sqrt{\pi}}\left(1-\frac{3}{4}\alpha+\frac{\pi}{8}\alpha\right)\langle\mathbf{nnr}\rangle_S+\frac{\alpha}{2\sqrt{\pi}}\langle\mathbf{1r}\rangle_S\right]\cdot\tilde{\boldsymbol{\nabla}}p, \tag{23h}$$

plus four contributions $\mathbf{F}[\bullet,\Delta\tilde{\boldsymbol{\omega}}_T]$ using the rule (19). All the 12 contributions to the torque are covered by the replacement rule (20). In this manuscript, we choose to neglect force and torque contributions nonlinear in the field gradients of the carrier gas. The quantity pA is proportional to a transport coefficient, as will be demonstrated in the examples below. In view of (23) it is thus apparent that all forces and torques are premultiplied with the transport coefficient, with the important exceptions being the terms proportional to the pressure gradients, $\boldsymbol{\nabla}p$ and $\tilde{\boldsymbol{\nabla}}p$. There is clearly a distinct origin of the effects of a pressure gradient compared to the other contributions.[1]

The compact result (23) supplemented with (19) and (20) is our main result for arbitrary convex geometries, and the surface integrals $\langle\cdots\rangle_S$ should be evaluated, and terms should be simplified *after* applying the replacement rules, but not earlier! This result is a particularly useful "intermediate" result because it clarifies the tensorial symmetries involved and therefore often allows to reduce the evaluation of a force contribution by calculating an integral with an integrand which just contains a single term rather than a sum. In order to avoid any confusion in interpreting the tensorial notation when applying the replacement rules (19) and (20), we notice that the μ component of the force contributions exhibit the forms $F_\mu[\bullet]=\langle C_\mu\rangle_S$ and $F_\mu[\bullet,\tilde{\mathbf{c}}_T]=c_\lambda\langle B_{\lambda\mu}\rangle_S$ with components $B_{\lambda\mu}$ and C_μ which do not depend on $\tilde{\mathbf{c}}_T$. Therefore, (19) and (20) yield $F_\mu[\bullet,\Delta\tilde{\boldsymbol{\omega}}_T]=-\epsilon_{\gamma\lambda\kappa}(\Delta\omega_T)_\kappa\langle r_\lambda B_{\gamma\mu}\rangle_S$, $T_\mu[\bullet]=\epsilon_{\mu\lambda\kappa}\langle C_\kappa r_\lambda\rangle_S$, $T_\mu[\bullet,\tilde{\mathbf{c}}_T]=\epsilon_{\mu\lambda\kappa}(\tilde{c}_T)_\gamma\langle B_{\gamma\kappa}r_\lambda\rangle_S$, and $T_\mu[\bullet,\Delta\tilde{\boldsymbol{\omega}}_T]=-\epsilon_{\mu\lambda\kappa}\epsilon_{\gamma\zeta\nu}(\Delta\omega_T)_\nu\langle r_\zeta B_{\gamma\kappa}r_\lambda\rangle_S$, where Einstein's summation applies. The results for the reduced levels of description, $\langle\boldsymbol{\phi}_1^1\rangle=\langle\boldsymbol{\phi}_0^2\rangle=\mathbf{0}$, can be read off from our result (23) by simply removing the corresponding terms.

For particles with three mutually perpendicular symmetry planes, integrals containing an odd-fold (pure or mixed) tensorial product of $\mathbf{r}$'s and $\mathbf{n}$'s vanish; thus exactly half of all contributions, such as $\mathbf{F}[0]$, $\mathbf{F}[\langle\boldsymbol{\phi}_0^2\rangle]$, and $\mathbf{T}[\tilde{\mathbf{c}}_T]$, to mention three of these 24 terms, vanish identically. We note that the forces $\mathbf{F}[\langle\boldsymbol{\phi}_1^1\rangle]$ and $\mathbf{F}[0,\tilde{\mathbf{c}}_T]$ in (23) require calculation of exactly the same surface integrals, as was noticed already, e.g., in Ref. 10. Using rule (20) we see that same holds for the torques $\mathbf{T}[\langle\boldsymbol{\phi}_1^1\rangle]$ and $\mathbf{T}[0,\tilde{\mathbf{c}}_T]$. A similar statement holds also for the forces $\mathbf{F}[\langle\boldsymbol{\phi}_0^2\rangle]$ and $\mathbf{F}[\langle\boldsymbol{\phi}_1^1\rangle,\tilde{\mathbf{c}}_T]$ containing $\langle\mathbf{nnn}\rangle_S$, and related torques which include a term of the form $\langle\mathbf{nnnr}\rangle_S$, respectively. These considerations further reduce the number of independent terms to be computed. Still, the number is large and we recently developed a code which allows to evaluate (23) using a symbolic programming language.[20]

The range of applicability of Grad's distribution (21) has been discussed,[31–34] and specifically also in the vicinity of boundaries.[35] The equilibrium Maxwell distribution is a trivial special case of (21). In the hydrodynamic approximation[26,36,37] the moments $\langle\boldsymbol{\phi}_k^n\rangle$ receive physical interpretation as follows:

$$\langle\boldsymbol{\phi}_1^1\rangle=\frac{2}{\sqrt{5}}\frac{\sqrt{\beta}\mathbf{q}}{p}=-\frac{3\sqrt{5}}{4}\frac{\eta}{p\sqrt{\beta}}\boldsymbol{\nabla}\ln T, \tag{24a}$$

$$\langle\boldsymbol{\phi}_0^2\rangle=\frac{1}{\sqrt{2}}\frac{\overline{\mathbf{p}}}{p}=-\sqrt{2}\frac{\eta\overline{\boldsymbol{\nabla}\mathbf{v}}}{p}, \tag{24b}$$

with heat flux $\mathbf{q}$, temperature T, macroscopic flow field $\mathbf{v}$ of the undisturbed solvent, hydrostatic pressure p, anisotropic (friction) pressure tensor $\overline{\mathbf{p}}$, solvent viscosity η, $\beta\equiv m_s/(2k_BT)$, Boltzmann's constant k_B, mass of a gas particle m_s, and the symbol $\overline{\ldots}$ denotes the symmetric traceless part of a tensor of arbitrary rank.[38,39] For a second rank tensor $\mathbf{p}$ one has $\overline{\mathbf{p}}=\frac{1}{2}(\mathbf{p}+\mathbf{p}^T)-p\mathbf{1}$ with $p=\frac{1}{3}\mathrm{Tr}(\mathbf{p})$. For an ideal gas made of rigid spheres of diameter d, the viscosity is explicitly given as[7,22,37] $\eta=\frac{5}{16}\sqrt{m_sk_BT/\pi}/d^2$ and $p=n_sk_BT$ with the particle number density n_s of the gas. Sometimes, the coefficient $\lambda\equiv\frac{15}{4}k_B/m_s$ is introduced to rewrite these relationships.

The main result of this section clearly highlights which surface integrals need to be computed to obtain the force and torque on the tracer particle, depending on which physical effects are accounted for. Most surface integrals in Eq. (23) do not depend on $\mathbf{r}$ but only on $\mathbf{n}$. In contrast, as soon as the torque is calculated or effects of particle rotation and pressure gradients are accounted for the surface integrals acquire additional dependencies on $\mathbf{r}$, and become substantially more difficult to compute (except for the case of a sphere). It is probably for that reason that theoretical calculations for these effects were only scarcely found in literature.

VIII. APPLICATIONS

A. ○ sphere

All normalized surface integrals $\langle\cdots\rangle_S$ in (23) for the forces and related expressions for torques (now denoted as $\langle\cdots\rangle_\bigcirc$ when treating a sphere) can be evaluated using the following result, valid for a sphere of radius R:

$$\begin{aligned}\langle(\otimes^\zeta\mathbf{r})(\otimes^x\mathbf{n})\rangle_\bigcirc&=R^\zeta\langle(\otimes^{x+\zeta}\mathbf{n})\rangle_S\\&=R^\zeta\frac{1}{2}\left(\frac{1+(-1)^{x+\zeta}}{1+x+\zeta}\right)[\mathbf{1}^{(x+\zeta)/2}]_{\mathrm{sym}},\end{aligned} \tag{25}$$

for all $\zeta,x\geqslant 0$, as demonstrated in Appendix B. The integral thus vanishes, as for any axisymmetric particle, for odd $(x+\zeta)$. Note that $[\mathbf{1}^0]_{\mathrm{sym}}=1$, $[\mathbf{1}^1]_{\mathrm{sym}}=\mathbf{1}$, $[\mathbf{1}^2]_{\mathrm{sym}}=(\mathbf{11}+\mathbf{i1i}+\mathbf{iii})/3$, etc. Equation (25) can be equivalently rewritten in a recursive fashion using $\langle 1\rangle_\bigcirc=1$, $\langle\mathbf{n}\rangle_\bigcirc=\mathbf{0}$,

$$\langle\mathbf{n}^{y+2}\rangle_\bigcirc=\frac{y+1}{y+3}[\langle\mathbf{n}^{y+2}\rangle_\bigcirc\mathbf{1}]_{\mathrm{sym}}, \tag{26}$$

for $y\geqslant 0$. The only difficulty when inserting (25) into (23) arises for terms of the form $[\mathbf{1nn}]_{\mathrm{sym}}$ or $[\mathbf{r1nnr}]_{\mathrm{sym}}$ as they appear in $\mathbf{F}[\langle\boldsymbol{\phi}_0^2\rangle]$ (23f) or $\mathbf{T}[\langle\boldsymbol{\phi}_0^2\rangle,\Delta\tilde{\boldsymbol{\omega}}_T]$, for example. There is some potential of further simplifying (23) using the fact that $\langle\boldsymbol{\phi}_0^2\rangle$ is symmetric and traceless, as demonstrated in detail in Appendix B.

We are now in the position to generalize a result recently derived[1] for purely translational degrees of freedom to the case of combined translational and rotational motions. With the area $A_\bigcirc=4\pi R^2$ and volume $V_\bigcirc=A_\bigcirc R/3$ of a sphere, and the coefficient

$$\tilde{\zeta}_\bigcirc\equiv\frac{4}{3\sqrt{\pi}}p_0A_\bigcirc, \tag{27}$$

with dimension of force (because $\tilde{\mathbf{c}}_T$ is dimensionless), we obtain the following contributions to the total force $\mathbf{F}$ on a sphere immersed in a nonequilibrium gas characterized by its first two tensorial moments $\langle\boldsymbol{\phi}_1^1\rangle$ and $\langle\boldsymbol{\phi}_0^2\rangle$;[40]

$$\mathbf{F}_\bigcirc[\langle\boldsymbol{\phi}_1^1\rangle]=\tilde{\zeta}_\bigcirc\frac{1}{2\sqrt{5}}\langle\boldsymbol{\phi}_1^1\rangle, \tag{28a}$$

$$\mathbf{F}_\bigcirc[\tilde{\boldsymbol{\nabla}}p]=-V_\bigcirc\boldsymbol{\nabla}p, \tag{28b}$$

$$\mathbf{F}_\bigcirc[0,\tilde{\mathbf{c}}_T]=-\tilde{\zeta}_\bigcirc\left(1+\frac{\pi}{8}\alpha\right)\tilde{\mathbf{c}}_T, \tag{28c}$$

$$\mathbf{F}_{\bigcirc}[\langle \boldsymbol{\phi}_0^2 \rangle, \tilde{\mathbf{c}}_T] = -\tilde{\zeta}_{\bigcirc} \frac{\sqrt{2}}{5} \langle \boldsymbol{\phi}_0^2 \rangle \cdot \tilde{\mathbf{c}}_T, \tag{28d}$$

$$\mathbf{F}_{\bigcirc}[\tilde{\boldsymbol{\nabla}} p, \Delta\tilde{\boldsymbol{\omega}}_T] = -V_{\bigcirc} \frac{\alpha R}{\sqrt{\pi}} \boldsymbol{\nabla}(\sqrt{\beta} p) \times \Delta\boldsymbol{\omega}_T. \tag{28e}$$

Correspondingly, using the replacement rules and some further calculations with the help of (23) and (26), we obtain the total torque $\mathbf{T}$ on a sphere as a sum of the three terms,

$$\mathbf{T}_{\bigcirc}[0, \Delta\tilde{\boldsymbol{\omega}}_T] = -\alpha \tilde{\zeta}_{\bigcirc} \frac{R^2}{2} \Delta\tilde{\boldsymbol{\omega}}_T, \tag{29a}$$

$$\mathbf{T}_{\bigcirc}[\langle \boldsymbol{\phi}_0^2 \rangle, \Delta\tilde{\boldsymbol{\omega}}_T] = \alpha \tilde{\zeta}_{\bigcirc} \left[\frac{R^2}{10\sqrt{2}} \langle \boldsymbol{\phi}_0^2 \rangle \cdot \Delta\tilde{\boldsymbol{\omega}}_T \right], \tag{29b}$$

$$\mathbf{T}_{\bigcirc}[\tilde{\boldsymbol{\nabla}} p, \tilde{\mathbf{c}}_T] = -V_{\bigcirc} \frac{\alpha R}{\sqrt{\pi}} \nabla(\sqrt{\beta} p) \times \tilde{\mathbf{c}}_T. \tag{29c}$$

All other force and torque contributions listed in (23) vanish due to symmetry.

The expression (28) for the force simplifies to known results upon neglecting angular motion, velocity, or pressure gradients.[1,10,11,16,23,26,28,41,42] When comparing with expressions available in the literature, one may replace $\langle \boldsymbol{\phi}_1^1 \rangle$ and $\langle \boldsymbol{\phi}_0^2 \rangle$ in the above equations by their hydrodynamic expressions (24). In (28e) and (29b) we inserted $\tilde{\boldsymbol{\nabla}} p$ following (13). Comparison of predicted forces and experimental data by Friedlander[43] for spherical particles yields $\alpha = 0.497$.

For the case of pure shear flow, if the tracer particle is moving in the direction of the flow lines, the force $\mathbf{F}_{\bigcirc}[\langle \boldsymbol{\phi}_0^2 \rangle, \tilde{\mathbf{c}}_T]$ tends to deflect the particle in the direction $\tilde{\mathbf{c}}_T \times (\boldsymbol{\nabla} \times \mathbf{v})$. This is opposite to the result of Saffman,[44,45] which is valid for dense highly viscous solvents and, particularly different from our treatment, stick boundary conditions at the particle surface are employed. We mention in that context that opposite signs have also been found for the Magnus effect for rotating particles immersed either in a dilute gas or in a continuum stream.[46,47] The term $\propto V_{\bigcirc} \nabla p$ is also worthy a note. It can be shown that, irrespective of the shape of the convex tracer particle of volume V, the term linear in field gradients always reads $-V\boldsymbol{\nabla} p$, termed "barodiffusion force"[19,48] which just follows from a balance of drag and inertia.[13] Even in the absence of pressure gradients the torque on a sphere does not vanish. Notice that the torque on a sphere vanishes for the case of purely elastic collisions, $\alpha = 0$.

B. □ Cube

For the case of a cubic tracer particle with square faces and edge length L, we can use a special case of the more general cuboidal shape treated in Appendix B to obtain the following normalized surface integrals:

$$\forall_{x=0,2,4,..} \langle (\otimes^x \mathbf{n}) \rangle_{\Box} = \frac{1}{3} \sum_{i=1}^{3} (\otimes^x \mathbf{e}_i), \tag{30a}$$

$$\forall_{x=1,3,5,..} \langle \mathbf{r} (\otimes^x \mathbf{n}) \rangle_{\Box} = \frac{L}{6} \sum_{i=1}^{3} (\otimes^{x+1} \mathbf{e}_i), \tag{30b}$$

$$\forall_{x=0,2,4,..} \langle \mathbf{rr} (\otimes^x \mathbf{n}) \rangle_{\Box} = \frac{5L^2}{36} \sum_{i=1}^{3} (\otimes^{x+2} \mathbf{e}_i). \tag{30c}$$

Inserting (30) into (23) with (19) and (20), restricting ourself to $\langle \boldsymbol{\phi}_0^2 \rangle = \mathbf{0}$, yields

$$\tilde{\zeta}_{\Box} \equiv \frac{4}{3\sqrt{\pi}} p A_{\Box}, \tag{31a}$$

$$\mathbf{F}_{\Box}[\langle \boldsymbol{\phi}_1^1 \rangle] = \frac{\tilde{\zeta}_{\Box}}{2\sqrt{5}} \langle \boldsymbol{\phi}_1^1 \rangle, \tag{31b}$$

$$\mathbf{F}_{\Box}[\tilde{\boldsymbol{\nabla}} p] = -V_{\Box} \boldsymbol{\nabla} p, \tag{31c}$$

$$\mathbf{F}_{\Box}[0, \tilde{\mathbf{c}}_T] = -\tilde{\zeta}_{\Box} \left(1 + \frac{\alpha\pi}{8}\right) \tilde{\mathbf{c}}_T, \tag{31d}$$

$$\mathbf{F}_{\Box}[\tilde{\boldsymbol{\nabla}} p, \Delta\tilde{\boldsymbol{\omega}}_T] = -\alpha V_{\Box} \frac{5}{6\sqrt{\pi}} L \Delta\tilde{\boldsymbol{\omega}}_T \times \tilde{\boldsymbol{\nabla}} p, \tag{31e}$$

$$\mathbf{T}_{\Box}[0, \Delta\tilde{\boldsymbol{\omega}}_T] = -\alpha \tilde{\zeta}_{\Box} \frac{5}{48} L^2 \Delta\tilde{\boldsymbol{\omega}}_T, \tag{31f}$$

$$\mathbf{T}_{\Box}[\tilde{\boldsymbol{\nabla}} p, \tilde{\mathbf{c}}_T] = -2A\tilde{\mathbf{c}}_T \cdot \left[\frac{2}{\sqrt{\pi}} \left(1 - \frac{3}{4}\alpha + \frac{\pi}{8}\alpha\right) \langle \mathbf{nnrr} \rangle_{\Box} + \frac{\alpha}{2\sqrt{\pi}} \langle \mathbf{rr} \rangle_{\Box} \right] \cdot \tilde{\boldsymbol{\nabla}} p, \tag{31g}$$

with $A_{\Box} = 6L^2$ and $V_{\Box} = L^3$, and all other force and torque contributions are equal to zero. The unevaluated surface integrals in (31g) are given by (30). These results compare well with the one for the sphere, mainly due to (30) where the identity $\mathbf{e}_1\mathbf{e}_1 + \mathbf{e}_2\mathbf{e}_2 + \mathbf{e}_3\mathbf{e}_3 = \mathbf{1}$ can be employed. The expression for the drag force $\mathbf{F}_{\Box}[0, \tilde{\mathbf{c}}_T]$ is identical to the one derived by Dahneke.[16]

C. ‖ cylindrical tube

We denote the orientation of the cylindrical tracer of radius R and height to diameter ratio Q by $\mathbf{e}_3$, cf. Fig. 1. We denote the length-to-radius ratio as $Q_{\parallel} = h/(2R)$. The surface area is $A_{\parallel} = 2\pi R^2 (1 + 2Q_{\parallel}) = A_{\bigcirc}(Q_{\parallel} + \frac{1}{2})$, volume $V_{\parallel} = \pi R^2 h = 2\pi R^3 Q_{\parallel}$. For symmetry reasons the forces (and also torques) onto a cylinder with symmetry axis $\mathbf{e}_3$ are invariant with respect to an exchange of $\mathbf{e}_1$ and $\mathbf{e}_2$ (as for the uniaxial ellipsoid), and we make use of the projector $\mathbf{P}_{\parallel} \equiv \mathbf{e}_3\mathbf{e}_3$ and of the expressions for the friction coefficient $\tilde{\zeta}_{\parallel}$ and the cylinder volume $V_{\parallel}$,

$$\tilde{\zeta}_{\parallel} \equiv 8\sqrt{\pi} p Q_{\parallel} R^2 = \frac{2(A_{\parallel}/A_{\bigcirc}) - 1}{\sqrt{\pi}} p A_{\bigcirc}, \tag{32}$$

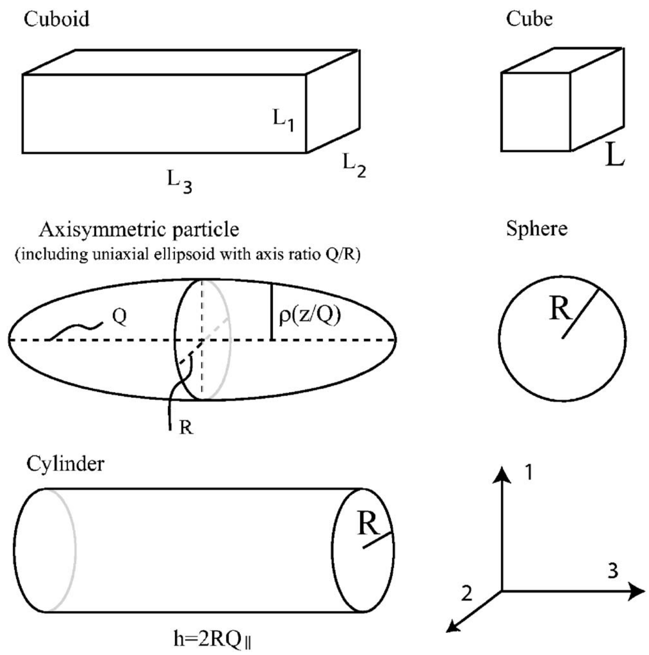

FIG. 1. Definition of quantities specifying the geometry of tracer particles. Top: cuboidal and cubic. Middle: axisymmetric with axis ratio Q/R and spherical. Bottom: cylindrical with flat end caps and length to diameter ratio $Q_\parallel$. Surface parametrizations are given in Table III.

$$V_\parallel = 2\pi Q_\parallel R^3, \tag{33}$$

to arrive, for $\langle \boldsymbol{\phi}_0^2 \rangle = \mathbf{0}$, at

$$\mathbf{F}_\parallel[\langle \boldsymbol{\phi}_1^1 \rangle] = \tilde{\zeta}_\parallel \frac{4-\alpha}{8\sqrt{5}} \langle \phi_1^1 \rangle - \tilde{\zeta}_\parallel \frac{4-3\alpha}{8\sqrt{5}} \mathbf{P}_\parallel \cdot \langle \phi_1^1 \rangle, \tag{34a}$$

$$\mathbf{F}_\parallel[\boldsymbol{\nabla} p] = - V_\parallel \boldsymbol{\nabla} p + V_\parallel \mathbf{P}_\parallel \cdot \boldsymbol{\nabla} p, \tag{34b}$$

$$\mathbf{F}_\parallel[0,\tilde{\mathbf{c}}_T] = - \tilde{\zeta}_\parallel \left(1 + \frac{\pi-2}{8}\alpha\right) \tilde{\mathbf{c}}_T + \tilde{\zeta}_\parallel \left(1 - \frac{6-\pi}{8}\alpha\right) \mathbf{P}_\parallel \cdot \tilde{\mathbf{c}}_T, \tag{34c}$$

$$\mathbf{F}_\parallel[\tilde{\boldsymbol{\nabla}} p, \Delta\tilde{\boldsymbol{\omega}}_T] = V_\parallel \frac{\alpha R}{\sqrt{\pi}} \tilde{\boldsymbol{\nabla}} p \times \Delta\tilde{\boldsymbol{\omega}}_T - V_\parallel \frac{R}{6\sqrt{\pi}} A^- (\mathbf{P}_\parallel \cdot \tilde{\boldsymbol{\nabla}} p) \times \Delta\tilde{\boldsymbol{\omega}}_T, \tag{34d}$$

$$\mathbf{T}_\parallel[0,\Delta\tilde{\boldsymbol{\omega}}_T] = - \tilde{\zeta}_\parallel \frac{R^2}{24} (A^+ \Delta\tilde{\boldsymbol{\omega}}_T - A^- \mathbf{P}_\parallel \cdot \Delta\tilde{\boldsymbol{\omega}}_T), \tag{34e}$$

$$\mathbf{T}_\parallel[\tilde{\boldsymbol{\nabla}} p, \tilde{\mathbf{c}}_T] = - V_\parallel \frac{\alpha R}{\sqrt{\pi}} (\tilde{\nabla} p \times \tilde{\mathbf{c}}_T) - V_\parallel \frac{R}{6\sqrt{\pi}} A^- ((\mathbf{P}_\parallel \cdot \tilde{\boldsymbol{\nabla}} p) \times \tilde{\mathbf{c}}_T), \tag{34f}$$

where the abbreviation $A^\pm \equiv 8Q_\parallel^2 + \alpha(\pi-2)Q_\parallel^2 \pm 6\alpha$ has been used. This is the result for a cylindrical tube without end caps when disregarding the second moment, $\langle \boldsymbol{\phi}_0^2 \rangle = \mathbf{0}$. Results in the presence of a velocity gradient can be obtained from (23) via algebraic manipulations.[20] Our result for the force contributions $\mathbf{F}_\parallel[0,\tilde{\mathbf{c}}_T]$ (34a)—and therefore also $\mathbf{F}_\parallel[\langle \boldsymbol{\phi}_1^1 \rangle]$ (34b)—exactly reduces to the one implicitly obtained earlier.[10] In (34), $\tilde{\boldsymbol{\nabla}} p$ throughout abbreviates $\beta^{-1/2} \boldsymbol{\nabla}(\beta^{1/2} p)$ as explained in (13). The hydrodynamic approximation (24) can be employed to rewrite (34) in terms of temperature, temperature gradients, heat flux, etc. The end caps (symbol $\cap$) are treated separately in the subsequent section (i) to facilitate the extension of the results to cylindrical particles with spherical end caps and (ii) to see, how the more general results for arbitrary axisymmetric particles to be discussed below simplify to the results for the simplest axisymmetric shape. The total force onto a cylindrical tracer with flat end caps is obtained by summation of the $\parallel$ and $\cap$ contributions.

D. ∩ flat end caps

The two flat end caps for the cylindrical tube are parametrized in Table III. The result for the two end caps (together) reads

$$\mathbf{F}_\cap[\langle \boldsymbol{\phi}_1^1 \rangle] = \tilde{\zeta}_\parallel \frac{\alpha}{8\sqrt{5}Q_\parallel} \langle \boldsymbol{\phi}_1^1 \rangle + \tilde{\zeta}_\parallel \frac{4-3\alpha}{8\sqrt{5}Q_\parallel} \mathbf{P}_\parallel \cdot \langle \boldsymbol{\phi}_1^1 \rangle, \tag{35a}$$

$$\mathbf{F}_\cap[\tilde{\boldsymbol{\nabla}} p] = - V_\parallel \mathbf{P}_\parallel \cdot \boldsymbol{\nabla} p, \tag{35b}$$

$$\mathbf{F}_\cap[0,\tilde{\mathbf{c}}_T] = - \frac{\tilde{\zeta}_\parallel}{Q_\parallel} \left\{ \frac{\alpha}{4}\mathbf{1} + \left[1 - \alpha\left(\frac{3}{4} - \frac{\pi}{8}\right)\right] \mathbf{P}_\parallel \right\} \cdot \tilde{\mathbf{c}}_T, \tag{35c}$$

$$\mathbf{F}_\cap[\tilde{\nabla} p, \Delta\tilde{\boldsymbol{\omega}}_T] = \frac{V_\parallel R}{\sqrt{\pi} Q_\parallel} \left\{ \frac{\alpha}{4} \tilde{\boldsymbol{\nabla}} p \times \Delta\tilde{\omega}_T - \frac{\alpha(1-4Q_\parallel^2)}{4} (\mathbf{P}_\parallel \cdot \tilde{\nabla} p) \times \Delta\tilde{\boldsymbol{\omega}}_T + \left[1 - \alpha\left(\frac{3}{4} - \frac{\pi}{8}\right)\right] \mathbf{P}_\parallel \cdot (\tilde{\boldsymbol{\nabla}} p \times \Delta\tilde{\boldsymbol{\omega}}_T) \right\}, \tag{35d}$$

$$\mathbf{T}_\cap[0,\Delta\tilde{\boldsymbol{\omega}}_T] = - \frac{\tilde{\zeta}_\parallel R^2}{4Q_\parallel} \left\{ \left[1 - \alpha\left(1 - \frac{\pi}{8} - Q_\parallel^2\right)\right] (\mathbf{1} - \mathbf{P}_\parallel) \cdot \Delta\tilde{\boldsymbol{\omega}}_T + \frac{\alpha}{2} \Delta\tilde{\boldsymbol{\omega}}_T \right\}, \tag{35e}$$

$$\mathbf{T}_\cap[\tilde{\boldsymbol{\nabla}} p, \tilde{\mathbf{c}}_T] = - \frac{V_\parallel R}{\sqrt{\pi} Q_\parallel} \left\{ \left[1 - \alpha\left(\frac{1}{2} - \frac{\pi}{8}\right)\right] ([(\mathbf{1} - \mathbf{P}_\parallel) \cdot \tilde{\boldsymbol{\nabla}} p] \times \tilde{\mathbf{c}}_T - \mathbf{P}_\parallel \cdot [\tilde{\boldsymbol{\nabla}} p \times \tilde{\mathbf{c}}_T]) + \alpha Q_\parallel^2 (\mathbf{P}_\parallel \cdot \tilde{\boldsymbol{\nabla}} p) \times \tilde{\mathbf{c}}_T + \frac{\alpha}{4} \mathbf{P}_\parallel \cdot (\tilde{\boldsymbol{\nabla}} p \times \tilde{\mathbf{c}}_T) \right\}, \tag{35f}$$

where $\mathbf{Q}_\parallel \equiv (\mathbf{1} - \mathbf{P}_\parallel)$. All other force and torque contributions not specified in (34) and (35) vanish due to symmetry, cf. Appendix B for details. The result for the drag force, (34c) plus (35c), agrees with the expression found by Dahneke.[16] In the limit $Q_\parallel \to \infty$, the drag force and the thermophoretic force, (34a) plus (35a), both agree with the expressions de-

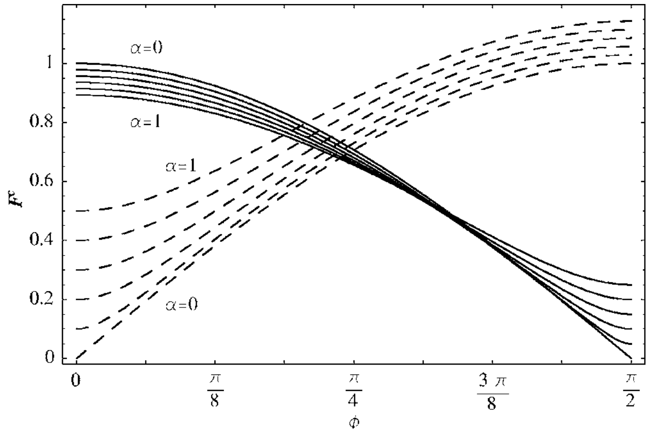

FIG. 2. Absolute value of the "friction" force $\mathbf{F}[0,\tilde{\mathbf{c}}_T]$ (34) and (35), made dimensionless by $\tilde{\zeta}_{\|}\tilde{c}_T/Q_{\|}$ for flat disks ($Q_{\|}\to 0$) (solid lines), and by $\tilde{\zeta}_{\|}\tilde{c}_T$ for long rods ($Q_{\|}\to\infty$) (dashed lines), respectively. The enclosed angle between the particles symmetry axis $\mathbf{e}_3$ and tracer velocity $\tilde{\mathbf{c}}_T$ ($\tilde{c}_T\equiv|\tilde{\mathbf{c}}_T|$) is denoted by ϕ. Results are shown vs ϕ for a range of accommodation coefficients equidistantly spaced between $\alpha=0$ (ideally elastic collision) $\alpha=1$ (ideally diffusive collision).

rived by García-Ybarra and Rosner[21] for a cylinder with spherical caps.[49] We point out that the drag force gets logarithmic corrections in the Knudsen number if at least one of the dimensions of the cylinder is larger than the mean free path in the carrier gas.[50] However, this a higher order effect not of interest in the "free molecular flow" limit studied here. It is noteworthy that the torque on the tracer particle also vanishes for $\alpha=0$.

Results for long rods ($Q_{\|}\to\infty$) and thin disks ($Q_{\|}\to 0$) obtained from the cylinder results (34) plus (35) converge to the ones for a rodlike and flat oblate ellipsoid, respectively, with half axis R. In the limit of flat disks, the dominant contributions are zeroth order in $Q_{\|}$. In contrast, for thin rods, the leading terms in the force and torque are cubic in $Q_{\|}$. Some illustrations of the forces are given in Figs. 2 and 3. For an artificial ensemble of randomly oriented cylinders

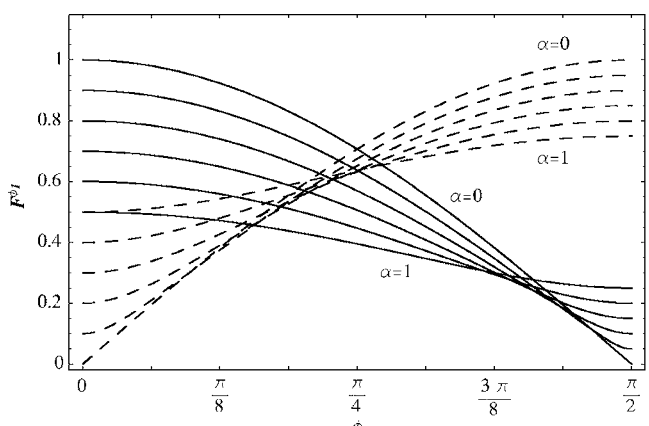

FIG. 3. Absolute value of the "thermophoretic" force $\mathbf{F}[\langle\boldsymbol{\phi}_1^1\rangle]$ (34) and (35) made dimensionless by $\tilde{\zeta}_{\|}|\langle\boldsymbol{\phi}_1^1\rangle|/(2\sqrt{5}Q_{\|})$ for flat disks ($Q_{\|}\to 0$) (solid lines), and by $\tilde{\zeta}_{\|}|\langle\boldsymbol{\phi}_1^1\rangle|/(2\sqrt{5})$ for long rods ($Q_{\|}\to\infty$) (dashed lines), respectively. The enclosed angle between the particles symmetry axis $\mathbf{e}_3$ and $\langle\boldsymbol{\phi}_1^1\rangle$ is denoted by ϕ. The strength $|\langle\boldsymbol{\phi}_1^1\rangle|$, in the hydrodynamic approximation, is proportional to the strength of the temperature gradient, cf. (24).

with $Q_{\|}=1$ one recovers, on average, all the expressions derived for the spherical tracer particle, cf. Sec. IX.

E. ⊖ axisymmetric particle

An axisymmetric, convex particle, directed along the $\mathbf{e}_3$ direction is parameterized by a radial function $\rho(v_2)$, where $v_2\in[-1,1]$, cf. Table III for its exact parametrization and the surface element $s(v_2)$. Its surface area reads

$$A_{\ominus}=2\pi\int s(v_2)dv_2=2\pi\int\rho(v_2)\sqrt{Q^2+\rho'(v_2)^2}dv_2. \tag{36}$$

Axisymmetric particles include the cylindrical tube, sphere, and uniaxial ellipsoid as special cases. The surface is closed if $\rho(-1)=\rho(1)=0$ and ρ smooth. Convexity of the particle is ensured if $\rho''\leqslant 0$. In this section we derive expressions for all surface integrals appearing in our expression for forces and torques (23), but we will not insert them in order to keep the manuscript short.

First, we notice from Table III that $\mathbf{r}$ and $\mathbf{n}$ can be written as $\mathbf{r}=X_{\mathbf{r}}\mathbf{e}^{iv_1}+Y_{\mathbf{r}}\mathbf{e}_3,\mathbf{n}=X_{\mathbf{n}}\mathbf{e}^{iv_1}+Y_{\mathbf{n}}\mathbf{e}_3$, with v_2-dependent functions $X_{\mathbf{r}}=\rho(v_2)$, $Y_{\mathbf{r}}=Qv_2$, $X_{\mathbf{n}}=Q/\sqrt{Q^2+\rho'^2}$, $Y_{\mathbf{n}}=\rho'/\sqrt{Q^2+\rho'^2}$, and thus

$$\langle(\otimes^n\bullet)\rangle_{\ominus}=\frac{A_{\|}}{2A}\sum_{k=0}^{n}\frac{n!}{k!(n-k)!}\left\{\frac{2}{A_{\|}}\int_0^{2\pi}[(\otimes^k\boldsymbol{e}^{\,\mathrm{i}v_1})dv_1\right\} \times(\otimes^{n-k}\mathbf{e}_3)]_{\mathrm{sym}}\int_{-1}^{1}X_\bullet^kY_\bullet^{n-k}s(v_2)dv_2 \tag{37}$$

for $\bullet\in\{\mathbf{r},\mathbf{n}\}$. In Eqs. (37), (38) and also (39a) the $\times$ symbol means "continue reading" and does not denote a cross product. While the last integral in (37) purely depends on the shape $\rho(v_2)$ of the tracer, the first integral between curly brackets [equals $\langle(\otimes^k\mathbf{n})\rangle_{\|}$ with $A_{\|}=4\pi Q$] has been already evaluated in connection with the cylindrical tracer (B6) for which $\mathbf{n}=\mathbf{e}^{iv_1}$. Thus (37) vanishes for odd n (and k is even too), and simplifies to

$$\langle(\otimes^n\bullet)\rangle_{\ominus}=\frac{A_{\|}}{2A}\sum_{k=0}^{n}\frac{n!}{k!(n-k)!}[\langle(\otimes^k\mathbf{n})\rangle_{\|} \times(\otimes^{(n-k)/2}\mathbf{P}_{\|})]_{\mathrm{sym}}\int_{-1}^{1}X_\bullet^kY_\bullet^{n-k}s\,dv_2, \tag{38}$$

where $\mathbf{P}_{\|}\equiv\mathbf{e}_3\mathbf{e}_3$ and $\langle(\otimes^2\mathbf{n})\rangle_{\|}=\frac{1}{2}(\mathbf{1}-\mathbf{P}_{\|})$, for example. We do not wish to elaborate on evaluating this expression further, but rather want to show how to apply it to obtain contributions to forces and torques which involve, for example, $\langle\mathbf{nn}\rangle_{\ominus}$ and $\langle\mathbf{nr}\rangle_{\ominus}$. Accordingly, evaluating (38) for $n=2$ and $\bullet=\mathbf{n}$ gives

$$\langle \mathbf{nn}\rangle_\ominus = \frac{A_\parallel}{2A_\ominus}\sum_{k=0,2}\frac{2}{k!(2-k)!}[\langle(\otimes^k\mathbf{n})\rangle_\parallel \times(\otimes^{(2-k)/2}\mathbf{P}_\parallel)]_{\mathrm{sym}}\int_{-1}^{1} X_{\mathbf{n}}^k Y_{\mathbf{n}}^{n-k} s dv_2 \tag{39a}$$

$$= \frac{4\pi Q}{2A_\ominus}\left[\mathbf{P}_\parallel\int_{-1}^{1} X_{\mathbf{n}}^0 Y_{\mathbf{n}}^2 s dv_2 + \frac{1}{2}(\mathbf{1}-\mathbf{P}_\parallel)\int_{-1}^{1} X_{\mathbf{n}}^2 Y_{\mathbf{n}}^0 s dv_2\right]$$

$$= \frac{4\pi Q}{2A_\ominus}\left[\mathbf{P}_\parallel\int_{-1}^{1}\frac{\rho'^2\rho}{\sqrt{Q^2+\rho'^2}}dv_2 + \frac{Q^2}{2}(\mathbf{1}-\mathbf{P}_\parallel)\int_{-1}^{1}\frac{\rho}{\sqrt{Q^2+\rho'^2}}dv_2\right], \tag{39b}$$

with A from (36). This result agrees with the calculations of Rotatschek and Zulehner[29] and Fernández de la Mora.[10]

We kept the term $Y_{\mathbf{n}}^0$ in (39a) because $Y_{\mathbf{n}}=0$ and $Y_{\mathbf{n}}^0=1$ for a cylindrical tube. For all other cases, we resubstituted $X_{\mathbf{n}}$ and $Y_{\mathbf{n}}$ according to their above definitions to obtain (39b). Correspondingly, from (39a) we immediately obtain, simply replacing $\mathbf{n}$ by $\mathbf{r}$,

$$\langle \mathbf{rr}\rangle_\ominus = \frac{4\pi Q}{2A}\left[Q^2\mathbf{P}_\parallel\int_{-1}^{1} v_2^2 s dv_2 + \frac{1}{2}(\mathbf{1}-\mathbf{P}_\parallel)\int_{-1}^{1}\rho^2 s dv_2\right], \tag{40}$$

again, with $s=\rho\sqrt{Q^2+\rho'^2}$. Finally, using the same approach, we have

$$\langle \mathbf{rn}\rangle_\ominus = \frac{4\pi Q}{2A}\left[\mathbf{P}_\parallel\int_{-1}^{1} Y_{\mathbf{n}}Y_{\mathbf{r}} s dv_2 + \frac{1}{2}(\mathbf{1}-\mathbf{P}_\parallel)\int_{-1}^{1} X_{\mathbf{n}}X_{\mathbf{r}} s dv_2\right]$$

$$= \frac{4\pi Q^2}{2A}\left[\mathbf{P}_\parallel\int_{-1}^{1} v_2\rho'\rho dv_2 + \frac{1}{2}(\mathbf{1}-\mathbf{P}_\parallel)\int_{-1}^{1}\rho^2 dv_2\right], \tag{41}$$

such that it should be transparent how to obtain all surface integrals appearing in our result for forces and torques, cf. Sec. VII. The above results valid for axisymmetric particles certainly reduce to the ones already stated for cylindrical tubes and spheres, when choosing $\rho(v_2)=R$ with constant R (a cylindrical tube), for which $X_r=R$, $Y_r=Qv_2$, $X_n=1$, $Y_n=0$, and $\rho=\sqrt{1-v_2^2}$ (for a sphere), see also Table III and Appendix B.

IX. ISOTROPIC PHASE

In order to simplify the general expressions to the case where an ensemble of axisymmetric particles is oriented isotropically (i.e., randomly), we employ the useful identities

$$\langle \mathbf{P}_\parallel\rangle^{\mathrm{iso}} = \tfrac{1}{3}\mathbf{1}, \tag{42a}$$

$$\langle \mathbf{P}_\parallel\mathbf{P}_\parallel\rangle^{\mathrm{iso}} = \tfrac{1}{5}[\mathbf{11}]_{\mathrm{sym}} = \tfrac{1}{15}(\mathbf{11}+\mathbf{i1i}+\mathbf{iiii}). \tag{42b}$$

These isotropic averages can be derived from more general expressions valid for the uniaxial phase, Eq. (4.2–3) in Ref. 51 or Eq. (10.38) in Ref. 38, for vanishing order parameters. We used the notation $\mathbf{1}=\mathbf{ii}$ to write the symmetric part in vector rather than component notation. In the isotropic phase the force contributions for a cylinder become

$$\mathbf{F}_\parallel^{\mathrm{iso}} = \frac{\tilde{\zeta}_\parallel}{6\sqrt{5}}\left(2+\frac{1}{Q_\parallel}\right)\langle\boldsymbol{\phi}_1^1\rangle - \frac{\tilde{\zeta}_\parallel}{3}\left(1+\frac{\pi}{8}\alpha\right)\left(2+\frac{1}{Q_\parallel}\right)\tilde{\mathbf{c}}_T + \cdots, \tag{43a}$$

etc., these expressions show strong similarities with the results for a sphere. After identifying the force coefficient $\tilde{\zeta}_\parallel$ with $\tilde{\zeta}_\bigcirc$ the isotropic averages (43) are identical to the corresponding expressions (28) for a spherical tracer particle for $Q_\parallel\to 1$. By virtue of (42a) alone, the same statement holds for the torque. For $Q_\parallel\neq 1$ the force still differs from the one for spheres, reflecting the net effect of shape on the phoretic motion.

X. CONCLUSIONS

In this manuscript we derived explicit expressions for both the forces and torques onto moving and rotating convex tracer particles for given velocity distribution function of the unperturbed, nonuniform rarefied gas. To derive the unifying expressions, we inserted the half-sphere integrals (A5) with (15) and the α tensors, (C8) with (C5) into forces and torques (1) with (11) and (12). We then obtained compact results valid for arbitrary convex tracer particles in terms of basic surface integrals, summarized in Sec. VII which include Grad's 13th moment approximation as a special case. Concerning geometries, we have then evaluated geometry-dependent integrals for the case of both axisymmetric and nonaxisymmetric particles. The corresponding forces and torques have been stated and discussed. They enter the equations of motion for tracer particles immersed in a nonequilibrium gas. We further showed how to modify the forces and torques for the case where a higher order expansion needs to be considered. And we reduced the problem of the calculation of forces and torques for arbitrarily shaped convex tracers to the calculation of normalized surface integral tensors (23) or $\boldsymbol{G}$ tensors (11), in general, a task which we are going to automatize based on the results of this manuscript to treat complex situations.[20] However, depending on the particle shape, a number of symmetry properties usually simplify this problem, as demonstrated here. Aerosol particles do not only experience the forces and torques as described in this manuscript. In addition, there are Brownian forces related to the calculated friction force by way of the fluctuation-dissipation theorem. Furthermore, there may be additional potential forces (e.g., gravitational, and buoyancy). These can be handled via a standard Brownian dynamics simulation or Fokker-Planck equation approach.[1,38,52–54] Only a few special cases of the results obtained here were spread in the literature. The presented unifying description allows us to extend the calculations to arbitrary convex shapes dissolved in an arbitrary nonuniform gas (beyond Grad's 13 moment approximation) conveniently.

ACKNOWLEDGMENTS

The authors acknowledge very helpful discussions with Pedro L. García-Ybarra, Santosh Ansumali, and Hans Christian Öttinger. This project has been supported through EU-NSF grant FP6-016375 (MNIBS) of the European Community.

APPENDIX A: HALF-SPHERE INTEGRALS

In order to perform the integration over half the unit sphere [Eq. (10)], we choose a parametrization of the unit vector $\mathbf{y}$ as follows: $\mathbf{y}=\Sigma_i y_i \mathbf{e}_i=\sqrt{1-z^2}(\cos\phi\,\mathbf{e}_1+\sin\phi\,\mathbf{e}_2)+z\mathbf{n}$, where $\mathbf{e}_1\cdot\mathbf{n}=\mathbf{e}_2\cdot\mathbf{n}=0$ and $\mathbf{n}$ is the symmetry axis of the half sphere. Then (10) is rewritten as

$$\boldsymbol{\Omega}_m=-\frac{1}{\pi}\int_0^{2\pi}\int_{-1}^{0}(\otimes^m\mathbf{y})z\,dz\,d\phi. \tag{A1}$$

We insert $\mathbf{y}$ into (A1) and use binomial coefficients to arrive at

$$\boldsymbol{\Omega}_m=-\frac{1}{\pi}\sum_{k=0}^{m}\sum_{l=0}^{k}\int_0^{2\pi}\int_{-1}^{0}y_1^l y_2^{k-l}z^{m-k+1}\times\frac{[(\otimes^l\mathbf{e}_1)(\otimes^{k-l}\mathbf{e}_2)(\otimes^{m-k}\mathbf{n})]_{\mathrm{sym}}}{l!(m-k)!(k-l)!/m!}dz\,d\phi, \tag{A2}$$

where $[\boldsymbol{A}]_{\mathrm{sym}}$ denotes a symmetrization of the tensor $\boldsymbol{A}$ in all its indices, including subsequent normalization. For example, $[(\otimes^2\mathbf{e}_1)(\otimes^1\mathbf{n})]_{\mathrm{sym}}=(\mathbf{e}_1\mathbf{e}_1\mathbf{n}+\mathbf{e}_1\mathbf{n}\mathbf{e}_1+\mathbf{n}\mathbf{e}_1\mathbf{e}_1)/3$. Making use of the identity $\mathbf{e}_1\mathbf{e}_1+\mathbf{e}_2\mathbf{e}_2+\mathbf{n}\mathbf{n}=\mathbf{1}$ allows us to rewrite (A2) as

$$\boldsymbol{\Omega}_m=-\frac{1}{\pi}\sum_{q=0}^{\mathrm{int}(m/2)}\frac{[(\otimes^q(\mathbf{1}-\mathbf{n}\mathbf{n}))(\otimes^{m-2q}\mathbf{n})]_{\mathrm{sym}}}{(2q)!(m-2q)!/m!}\times\int_0^{2\pi}\int_{-1}^{0}y_1^{2q}z^{m-2q+1}dz\,d\phi, \tag{A3}$$

where int $(m/2)$ denotes the integer part of $m/2$. The integral can be evaluated explicitly as follows:

$$\frac{1}{\pi}\int_0^{2\pi}\int_{-1}^{0}y_1^{2q}z^{m-2q+1}dz\,d\phi=\frac{(-1)^{m+1}\left(q-\frac{1}{2}\right)![(m/2)-q]!}{[1+(m/2)]!\sqrt{\pi}}, \tag{A4}$$

where $x!$ is evaluated with the gamma function as $x!=\Gamma(x+1)$. Finally, $\boldsymbol{\Omega}_m$ is a linear combination of mixed, symmetric tensors of the kind $[(\otimes^k\mathbf{1})(\otimes^{m-2k}\mathbf{n})]_{\mathrm{sym}}$ and we can introduce numerical coefficients given in (15) of Sec. V of this manuscript in order to write down our explicit result for the $\boldsymbol{\Omega}_n$ tensors of arbitrary rank $m\geqslant 0$ as

$$\boldsymbol{\Omega}_m=\sum_{p=0}^{\mathrm{int}(m/2)}c_m^p[(\otimes^p\mathbf{1})(\otimes^{m-2p}\mathbf{n})]_{\mathrm{sym}}, \tag{A5}$$

which proves (14).

APPENDIX B: BASIC SURFACE INTEGRALS VIA SYMMETRY CONSIDERATIONS

As we have shown in Sec. VII, alculating forces and torques for arbitrary distribution functions (of tensorial order M) effectively requires, for any given shape of the tracer, not more than the evaluation of the following basic surface integrals:

$$\langle(\otimes^n\mathbf{r})(\otimes^x\mathbf{n})(\otimes^z\mathbf{r})\rangle_S\equiv\frac{1}{A}\int(\otimes^n\mathbf{r})(\otimes^x\mathbf{n})(\otimes^z\mathbf{r})dS, \tag{B1}$$

for $n\in\{0,1\}$, $x\in\{0,1,2,..,M+1\}$, and $z\in\{0,1\}$ and for $n=2$, $x\in\{0,1,2,3\}$, and $z\in\{0,1\}$ which results from (12), (11), and (7) together with the assumption $\tilde{c}_T\ll c$. Of course, by just changing indices, it is then sufficient to calculate the following integrals:

$$\langle(\otimes^\zeta\mathbf{r})(\otimes^x\mathbf{n})\rangle_S\equiv\frac{1}{A}\int(\otimes^\zeta\mathbf{r})(\otimes^x\mathbf{n})dS, \tag{B2}$$

with $\zeta\in\{0,1,2,3\}$ and $x\in\{0,1,2,..,M+1\}$ covering all cases (B1). In the following we will evaluate the integrals (B1) or equivalently (B2) for some geometries (the axisymmetric particle is treated in Sec. VIII E). With these expressions at hand, the forces and torques are available through (23) which contain the still unevaluated integrals. To us it seems that this approach provides the most compact and transparent presentation of explicit results, while at the same time facilitating the generalization to other geometries.

In order to get a flair on how to make use of this appendix, let us show why the following contributions to the torque vanish: (i) $\mathbf{T}[\langle\boldsymbol{\phi}_0^2\rangle]$ for a sphere, (ii) $\mathbf{T}[0]$ for a cylinder, and (iii) $\mathbf{T}[\langle\boldsymbol{\phi}_1^1\rangle,\tilde{\mathbf{c}}_T]$ for a cube. Case (i): according to (23) with (20) we have $\mathbf{T}[\langle\boldsymbol{\phi}_0^2\rangle]=c_1\boldsymbol{\epsilon}:(\langle\boldsymbol{\phi}_0^2\rangle:\langle\mathbf{nnnr}\rangle_S)+c_2\boldsymbol{\epsilon}:(\langle\boldsymbol{\phi}_0^2\rangle:\langle[\mathbf{1n}]_{\mathrm{sym}}\mathbf{r}\rangle_S$ with constant coefficients $c_{1,2}$, to be evaluated for a sphere. Here, $\langle\mathbf{nnnr}\rangle_{\bigcirc}\propto\langle\mathbf{nnnn}\rangle_{\bigcirc}$ [due to Eq. (B3)] which is symmetric in the last two indices, $\boldsymbol{\epsilon}:\mathbf{A}$ vanishes if $\mathbf{A}$ is symmetric, and thus the term with c_1 vanishes. Similarly, $\langle\boldsymbol{\phi}_0^2\rangle:\langle[\mathbf{1n}]_{\mathrm{sym}}\mathbf{r}\rangle_{\bigcirc}\propto\langle\boldsymbol{\phi}_0^2\rangle:\langle(\mathbf{1nn}+\mathbf{inin}+\mathbf{niin})\rangle_{\bigcirc}$ simplifies to $2\langle\boldsymbol{\phi}_0^2\rangle$ (which is again symmetric) because $\langle\boldsymbol{\phi}_0^2\rangle$ is also traceless by definition, $(\langle\boldsymbol{\phi}_0^2\rangle:\mathbf{1}=0)$, and $\langle\mathbf{nn}\rangle\propto\mathbf{1}$ [due to Eq. (B4)]. Case (ii): we derived $\mathbf{T}[0]\propto\boldsymbol{\epsilon}:\langle\mathbf{nr}\rangle_S$ for arbitrary geometries. For a cylinder, $\mathbf{r}=c_1\mathbf{n}+c_2 v_2\mathbf{e}_3$ holds (cf. Table III), thus $\mathbf{T}[0]\propto\boldsymbol{\epsilon}:\langle\mathbf{n}v_2\rangle_{\|}\mathbf{e}_3$ since $\mathbf{nn}$ is symmetric and does not contribute. Finally, because $\mathbf{n}$, for a cylinder, is independent of v_2 and $v_2\in[-1,1]$ (torque with respect of center of mass for a homogeneous cylinder), the surface integral vanishes. Case (iii): we have $\mathbf{T}[\langle\boldsymbol{\phi}_1^1\rangle,\tilde{\mathbf{c}}_T]\propto\boldsymbol{\epsilon}:[\langle\boldsymbol{\phi}_1^1\rangle\cdot(\tilde{\mathbf{c}}_T\cdot\langle\mathbf{nnnr}\rangle_S)]$, in general. For a cube, $\langle\mathbf{nnnr}\rangle_{\square}\propto\Sigma_{i=1}^3 L_i(\otimes^4\mathbf{e}_i)$ [using Eq. (B20)] is symmetric in the last two indices (to be double contracted with the antisymmetric $\boldsymbol{\epsilon}$) and thus vanishes.

1. ○ sphere of radius *R*

The surface of a sphere of radius R is parametrized by $\mathbf{r}=R\mathbf{n}$, normal vector $\mathbf{n}=(\cos v_1\mathbf{e}_1+\sin v_1\mathbf{e}_2)\sqrt{1-v_2^2}+v_2\mathbf{e}_3$ with $v_1\in[0,2\pi]$, $v_2\in[-1,1]$, and surface element $s=R^2$, cf. Table III. Accordingly, surface area $A=\int dS=4\pi R^2$. Since

$$\langle(\otimes^\zeta\mathbf{r})(\otimes^x\mathbf{n})\rangle_{\bigcirc}=R^\zeta\langle(\otimes^{x+\zeta}\mathbf{n})\rangle_{\bigcirc} \tag{B3}$$

holds, the task is reduced towards calculating the symmetric tensor $\langle(\otimes^x\mathbf{n})\rangle_{\bigcirc}$. For a sphere this tensor is certainly isotropic, i.e., $\langle(\otimes^y\mathbf{n})\rangle_{\bigcirc}\propto[\mathbf{1}^{y/2}]_{\mathrm{sym}}$, and (thus) vanishes for odd y

$=x+\zeta$. We hence need to calculate the coefficient of proportionality, or equivalently, a single component of the tensor. We choose the "simplest" component, which is $\langle n_3^y\rangle_\bigcirc$, with $n_3\equiv\mathbf{n}\cdot\mathbf{e}_3=v_2$, and obtain

$$\langle n_3^y\rangle_\bigcirc=\langle v_2^x\rangle_\bigcirc=\frac{1}{A}\int v_2^y s dv_1 dv_2 =\frac{1}{2}\int v_2^y dv_2=\frac{1}{2}\left(\frac{1+(-1)^y}{1+y}\right),$$

which provides the solution to the task (B2) for the sphere as follows:

$$\langle(\otimes^\zeta\mathbf{r})(\otimes^x\mathbf{n})\rangle_\bigcirc=R^\zeta\frac{1}{2}\left(\frac{1+(-1)^{x+\zeta}}{1+x+\zeta}\right)[\mathbf{1}^{(x+\zeta)/2}]_{\text{sym}}. \tag{B4}$$

Note that $[\mathbf{1}^0]_{\text{sym}}=1$, $[\mathbf{1}^1]_{\text{sym}}=\mathbf{1}$, $[\mathbf{1}^2]_{\text{sym}}=(\mathbf{11}+\mathbf{i1i}+\mathbf{iiii})/3$, etc. Equation (B4) can be equivalently rewritten in a recursive fashion using $\langle 1\rangle_\bigcirc=1$, $\langle\mathbf{n}\rangle_\bigcirc=\mathbf{0}$, $\langle\mathbf{n}^{y+2}\rangle_\bigcirc=(y+1)(y+3)^{-1}[\langle\mathbf{n}^{y+2}\rangle_\bigcirc\mathbf{1}]_{\text{sym}}$ for $y\geqslant 0$.

2. ‖ cylindrical tube of radius *R* and height $h=2RQ_\parallel$

Here, $\mathbf{r}/R=\cos v_1\mathbf{e}_1+\sin v_1\mathbf{e}_2+Q_\parallel v_2\mathbf{e}_3$ with $v_1\in[0,2\pi]$ and $v_2\in[-1,1]$, thus $\mathbf{n}=\cos v_1\mathbf{e}_1+\sin v_1\mathbf{e}_2$, $s=R$, $A=4\pi R^2 Q_\parallel$, $V=\pi R^2 h=2\pi R^3 Q_\parallel$, and height to diameter ratio $Q_\parallel$. Again, we take into account a basic symmetry consideration to evaluate (B2) and trace integrals with $\zeta>0$ or $z>0$ back to integrals of lower rank, in the light of the representation $\mathbf{r}=R(\mathbf{n}+v_2 Q_\parallel\mathbf{e}_3)$. All integrals can be rewritten in terms of $\mathbf{1}$ and $\mathbf{p}_\parallel\equiv\mathbf{e}_3\mathbf{e}_3$ since $\mathbf{p}_\parallel=\mathbf{1}-\mathbf{e}_1\mathbf{e}_2-\mathbf{e}_2\mathbf{e}_2$. These considerations lead, for $x=2$ and $x=4$, for example, to the ansatz

$$\langle(\otimes^2\mathbf{n})\rangle_\parallel=c_1\mathbf{1}+c_2\mathbf{P}_\parallel, \tag{B5}$$

$$\langle(\otimes^4\mathbf{n})\rangle_\parallel=d_1[\mathbf{11}]_{\text{sym}}+d_2[\mathbf{1P}_\parallel]_{\text{sym}}+d_3[\mathbf{P}_\parallel\mathbf{P}_\parallel]_{\text{sym}}, \tag{B6}$$

where the coefficients are manually calculated, cf. previous section, via

$$c_1=\langle n_1^2\rangle_\parallel=\langle\cos^2 v_1\rangle_\parallel=\tfrac{1}{2},$$

$$c_2=\langle n_3^2\rangle_\parallel-c_1=-c_1,$$

$$d_1=\langle n_1^4\rangle_\parallel=\langle\cos^4 v_1\rangle_\parallel=\tfrac{3}{8},$$

$$d_2=\langle n_3^2 n_1^3\rangle_\parallel-d_1=(c_1+c_2)c_1-d_1=-d_1,$$

$$d_3=\langle n_3^4\rangle_\parallel-d_1-d_2=-d_1-d_2=0, \tag{B7}$$

and so on for $x\geqslant 6$. Further, we have, for the cylindrical tube, using $\mathbf{r}=R(\mathbf{n}+v_2Q_\parallel\mathbf{e}_3)$,

$$\langle\mathbf{r}(\otimes^x\mathbf{n})\rangle_\parallel=R\langle(\otimes^{x+1}\mathbf{n})\rangle_\parallel, \tag{B8}$$

because $\langle v_2(\otimes^x\mathbf{n})\rangle_\parallel=\langle v_2\rangle\langle(\otimes^x\mathbf{n})\rangle_\parallel=0$,

$$\langle\mathbf{rr}(\otimes^x\mathbf{n})\rangle_\parallel=R^2\langle(\mathbf{n}+v_2Q_\parallel\mathbf{e}_3)(\mathbf{n}+v_2Q_\parallel\mathbf{e}_3)(\otimes^x\mathbf{n})\rangle_\parallel =R^2\left[\langle(\otimes^{x+2}\mathbf{n})\rangle_\parallel+\frac{Q_\parallel^2}{3}\mathbf{P}_\parallel\langle(\otimes^x\mathbf{n})\rangle_\parallel\right], \tag{B9}$$

where the denominator stems from $\langle v_2^2\rangle_\parallel=\frac{1}{3}$ and, analogously,

$$\langle\mathbf{rr}(\otimes^x\mathbf{n})\mathbf{r}\rangle_\parallel=R^3(\otimes^{x+3}\mathbf{n})+\frac{R^3Q_\parallel^2}{3}[\mathbf{P}_\parallel\langle(\otimes^{x+1}\mathbf{n})\rangle_\parallel +\mathbf{e}_3\langle(\otimes^{x+1}\mathbf{n})\rangle_\parallel\mathbf{e}_3+\langle\mathbf{ne}_3(\otimes^x\mathbf{n})\rangle_\parallel\mathbf{e}_3]. \tag{B10}$$

We have thus traced back all integrals (B2) to the the integral $\langle(\otimes^x\mathbf{n})\rangle_\parallel$ for which a closed form solution can be written down as a series in terms of integrals of the form $\langle[(\otimes^n\mathbf{1})(\otimes^m\mathbf{P}_\parallel)]_{\text{sym}}\rangle_\parallel$. Because it will be often sufficient for practical purposes, we presented the alternate recursive approach (B6) with (B7).

3. ∩ flat end caps for cylinder of radius *R* and height $h=2RQ_\parallel$

The two end caps are parametrized by $\mathbf{r}/R=\mp v_2\cos v_1\mathbf{e}_1+v_2\sin v_1\mathbf{e}_2\pm Q_\parallel\mathbf{e}_3$, $v_1\in[0,2\pi]$ and $v_2\in[-1,1]$, yielding $\mathbf{n}=\pm\mathbf{e}_3$ and $s=R^2|v_2|$. To make use of the results we prefer using the area $A=4\pi R^2Q_\parallel$ of the cylinder when normalizing the integrals. Thus

$$\langle(\otimes^x\mathbf{n})\rangle_\cap=\frac{1}{A}[1+(-1)^x](\otimes^x\mathbf{e}_3)\int R^2|v_2|dv_2dv_1 =\frac{[1+(-1)^x]}{2Q_\parallel}(\otimes^x\mathbf{e}_3)=\frac{1}{Q_\parallel}(\otimes^{x/2}\mathbf{P}_\parallel), \tag{B11}$$

$$\langle\mathbf{r}(\otimes^x\mathbf{n})\rangle_\cap=\mathbf{0}, \tag{B12}$$

$$\langle\mathbf{rr}(\otimes^x\mathbf{n})\rangle_\cap=\frac{R^4}{A}[\pi(\mathbf{1}-\mathbf{P}_\parallel)+4\pi Q_\parallel^2\mathbf{P}_\parallel](\otimes^{x/2}\mathbf{P}_\parallel), \tag{B13}$$

$$\langle\mathbf{rrr}(\otimes^x\mathbf{n})\rangle_\cap=\mathbf{0}, \tag{B14}$$

where it is understood that $(\otimes^{x/2}\mathbf{p}_\parallel)$ vanishes if x is odd.

4. □ cuboid of size $L_{1,2,3}$

A cuboid oriented along the $\mathbf{e}_{1,2,3}$ axes has six faces which we shall denote as $F=123$, $F=132$, $F=213$, $F=231$, $F=312$, and $F=321$ to simplify the analysis. Doing so, face $F=\mu\nu\kappa$ of the cuboid is parametrized by

$$\mathbf{r}^{(F)}=\epsilon_{\mu\nu\kappa}\left(\frac{L_\mu}{2}\mathbf{e}_\mu+v_1\frac{L_\nu}{2}\mathbf{e}_\nu+v_2\frac{L_\kappa}{2}\mathbf{e}_\kappa\right), \tag{B15}$$

where a summation convention is *not* used, $\epsilon_{\mu\nu\kappa}$ are the components of the Levi-Civita tensor, and $v_1\in[-1,1]$ and $v_2\in[-1,1]$. From (B15) we immediately derive the normal vector $\mathbf{n}^{(F)}=\epsilon_{\mu\nu\kappa}\mathbf{e}_\mu$ and surface element $s^{(F)}=L_\nu L_\kappa/4$ for face F. The area and volume of a cuboid are $A=\int dS=2(L_1L_2+L_1L_3+L_2L_3)$ and $V=L_1L_2L_3$, respectively. Unlike for the sphere, for which $\mathbf{r}\propto\mathbf{n}$, we cannot simplify the task (B2) in a fashion corresponding to the case of a sphere. We have to go through a more tedious calculation. For the single face $F=\mu\nu\kappa$ we have $\int dS^{(F)}=\int s^{(F)}dv_1dv_2=4s^{(F)}=L_\nu L_\kappa$, and we have to sum over

$$\langle(\otimes^x\mathbf{n})\rangle_\square^{(F)}=\frac{1}{A}\epsilon_{\mu\nu\kappa}^x(\otimes^x\mathbf{e}_\mu)\int dS^{(F)}=\frac{1}{A}\epsilon_{\mu\nu\kappa}^x(\otimes^x\mathbf{e}_\mu)L_\nu L_\kappa, \tag{B16}$$

where $\epsilon_{\mu\nu\kappa}^x$ denotes the xth power of the number $\epsilon_{\mu\nu\kappa}$, and

$$\langle \mathbf{r}(\otimes^x \mathbf{n})\rangle_{\Box}^{(F)} = \frac{1}{A}\epsilon^{1+x}_{\mu\nu\kappa}\int\left(\frac{L_\mu}{2}\mathbf{e}_\mu + v_1\frac{L_\nu}{2}\mathbf{e}_\nu + v_2\frac{L_\kappa}{2}\mathbf{e}_\kappa\right) \times(\otimes^x \mathbf{e}_\mu)dS^{(F)} = \frac{V}{2A}\epsilon^{1+x}_{\mu\nu\kappa}(\otimes^{1+x}\mathbf{e}_\mu), \qquad \text{(B17)}$$

etc. for all faces (notice: $\times$ in (B17) is not a cross product) to arrive at $\forall_{x=1,3,5,..}\langle(\otimes^x\mathbf{n})\rangle_\Box=0$, because (B16) is symmetric in $\nu\kappa$ and

$$\langle(\otimes^x\mathbf{n})\rangle_\Box = \sum_{\mu,\nu,\kappa=1}^{3}\langle(\otimes^x\mathbf{n})\rangle_\Box^{(F)} = \frac{2}{A}[(\otimes^x\mathbf{e}_1)L_2L_3 + (\otimes^x\mathbf{e}_2)L_3L_1 + (\otimes^x\mathbf{e}_3)L_1L_2], \qquad \text{(B18)}$$

for even $x \geqslant 0$. More generally, we find

$$\langle(\otimes^\zeta\mathbf{r})(\otimes^x\mathbf{n})\rangle_\Box = 0 \quad \text{if } \zeta + x \text{ is odd.} \qquad \text{(B19)}$$

Further, while skipping intermediate steps, we arrive at

$$\langle\mathbf{r}(\otimes^x\mathbf{n})\rangle_\Box = \frac{V}{A}\sum_{i=1}^{3}(\otimes^{1+x}\mathbf{e}_i), \qquad \text{(B20)}$$

for odd $x \geqslant 1$, and

$$\langle\mathbf{rr}(\otimes^x\mathbf{n})\rangle_\Box = \frac{1}{12}\sum_{i=1}^{3}L_i^2(\otimes^{x+2}\mathbf{e}_i) + \frac{V}{3A}\sum_{i=1}^{3}L_i(\otimes^{x+2}\mathbf{e}_i), \qquad \text{(B21)}$$

for even $x \geqslant 0$, where $\mathbf{e}_4 \equiv \mathbf{e}_1$ and $\mathbf{e}_5 \equiv \mathbf{e}_2$ have been introduced to simplify notation and finally, Eqs. (B18)–(B21) are the solutions to all tasks posed by (B2) except the one for $\langle\mathbf{r}^2(\otimes^x\mathbf{n})\mathbf{r}\rangle_\Box$ which we refrain from writing down, albeit conceptually as "simple" to obtain as the stated results.

APPENDIX C: ORTHONORMAL EXPANSION AND α TENSORS

Any velocity distribution function $f(\mathbf{c})$ can be expanded in terms of orthonormal (scalar product defined by f_0), dimensionless moments $\boldsymbol{\phi}_k^n(\mathbf{c})$ as follows:

$$f(\mathbf{c}) = f_0(\mathbf{c})\left(1 + \sum_{n,k}^{\infty}\langle\boldsymbol{\phi}_k^n\rangle\odot^n\boldsymbol{\phi}_k^n\right), \qquad \text{(C1)}$$

where $f_0(\mathbf{c})$ denotes the isotropic part of the distribution function, and the average is defined as

$$\langle\boldsymbol{\phi}_k^n\rangle = n_s^{-1}\int f(\mathbf{c})\boldsymbol{\phi}_k^n d^3\mathbf{c}, \qquad \text{(C2)}$$

with particle number density n_s for convenience, because $\mathbf{c}$ will have dimension of velocity and the spatially averaged f should be dimensionless. The isotropy of f_0 requires that $\boldsymbol{\phi}$'s are linear in the irreducible tensors made of $\mathbf{c}$'s. For the case that $f_0 \propto e^{-\tilde{c}^2}$, more precisely, $f_0(\mathbf{c})=n_s(\beta/\pi)^{3/2}e^{-\tilde{c}^2}$ with $\tilde{\mathbf{c}}=\sqrt{\beta}\mathbf{c}$ and $\tilde{c}=|\tilde{\mathbf{c}}|$, the orthonormal polynomials are the associated Laguerre (or Sonine) functions L_k^n defined as

$$L_k^m(x) = \sum_{i=0}^{k}\frac{(k+m)!}{i!(k-i)!(m+i)!}(-x)^i, \qquad \text{(C3)}$$

i.e., $L_0^m=1$, $L_1^{3/2}(x)=\frac{5}{2}-x$, and we have

$$\boldsymbol{\phi}_k^n = l_k^n L_k^{n+1/2}(\tilde{c}^2)\overline{\otimes^n\tilde{\mathbf{c}}}, \quad l_k^n \equiv \left(\frac{\sqrt{\pi}}{2}\frac{k!(1+2n)!!}{(k+n+(1/2))!n!}\right)^{1/2}. \qquad \text{(C4)}$$

The normalization coefficients arise from the orthogonality features of the Laguerre functions, $\int_0^\infty e^{-x}x^m L_k^m(x)L_{k'}^m(x)dx = \delta_{k,k'}(k+m)!/k!$, and the one for irreducible tensors, $\int_{S_1}\overline{\otimes^n\hat{\mathbf{c}}}\,\overline{\otimes^m\hat{\mathbf{c}}}d^2\hat{c}=4\pi\delta_{n,m}n!/(2n+1)!!\boldsymbol{\Delta}^{(\mathbf{n})}$, where $\boldsymbol{\Delta}^{(\mathbf{n})}$ is a projector with the feature[38] $\boldsymbol{\Delta}^{(\mathbf{n})}(\otimes^{\mathbf{n}}\hat{\mathbf{c}})=\overline{\otimes^n\hat{\mathbf{c}}}$. The symbol $\hat{\mathbf{c}}$ denotes the unit vector $\mathbf{c}/c$. The lowest order "moments" therefore are given by (22). We should mention that the requirements $\langle\mathbf{c}\rangle=\mathbf{0}$ and $m_s/2\langle c^2\rangle=\frac{3}{2}k_BT$ immediately yield $\langle\boldsymbol{\phi}_1^0\rangle=0$ and $\langle\boldsymbol{\phi}_0^1\rangle=0$. The remaining two lowest order moments are then $\langle\boldsymbol{\phi}_1^1\rangle$ and $\langle\boldsymbol{\phi}_0^2\rangle$. Assuming $a \ll c$, thus neglecting terms of order $(a/c)^{>1}$, we have

$$\begin{aligned}
f(\mathbf{c}+\mathbf{a}) &= f_0(\mathbf{c}+\mathbf{a})\sum_{n,k=0}^{\infty}\langle\boldsymbol{\phi}_k^n\rangle\odot^n\boldsymbol{\phi}_k^n(\mathbf{c}+\mathbf{a}) \\
&\overset{a\ll c}{\approx} f_0(\mathbf{c})(1-2\tilde{\mathbf{c}}\cdot\tilde{\mathbf{a}})\sum_{n,k}l_k^n L_k^{n+(1/2)}(\tilde{c}^2+2\tilde{\mathbf{c}}\cdot\tilde{\mathbf{a}}) \\
&\quad\times(n\overline{\tilde{\mathbf{a}}(\overline{\otimes^{n-1}\tilde{\mathbf{c}}})}+\overline{\otimes^n\tilde{\mathbf{c}}})\odot^n\langle\boldsymbol{\phi}_k^n\rangle \\
&= f_0(\mathbf{c})\Bigg[\sum_{n,k}l_k^n L_k^{n+(1/2)}(\tilde{c}^2)\Bigg(n\overline{\tilde{\mathbf{a}}(\overline{\otimes^{n-1}\tilde{\mathbf{c}}})} \\
&\quad+3\left(1-\frac{2}{3}\tilde{\mathbf{c}}\cdot\tilde{\mathbf{a}}\right)\overline{\otimes^n\tilde{\mathbf{c}}}\Bigg)\odot^n\langle\boldsymbol{\phi}_k^n\rangle \\
&\quad+2\tilde{\mathbf{c}}\cdot\tilde{\mathbf{a}}\sum_{n,k}l_k^n\sum_{i=0}^{k}\frac{(k+n+(1/2))!}{(i-1)!(k-i)!(n+i+(1/2))!} \\
&\quad\times(-\tilde{c}^2)^i\overline{\otimes^n\tilde{\mathbf{c}}}\odot^n\langle\boldsymbol{\phi}_k^n\rangle\Bigg],
\end{aligned} \qquad \text{(C5)}$$

where we used the notation $\tilde{\mathbf{a}}=(\tilde{c}/c)\mathbf{a}$ and the following result:

$$\begin{aligned}
L_k^m(\tilde{c}^2+2\tilde{\mathbf{a}}\cdot\tilde{\mathbf{c}}) &\overset{a\ll c}{\approx}\sum_{i=0}^{k}\frac{(k+m)!}{i!(k-i)!(m+i)!}(-\tilde{c}^2)^i(1+2i\tilde{\mathbf{a}}\cdot\tilde{\mathbf{c}}) \\
&= L_k^m(\tilde{c}^2)+2\sum_{i=0}^{k}\frac{(k+m)!}{(i-1)!(k-i)!(m+i)!} \\
&\quad\times(-\tilde{c}^2)^i\tilde{\mathbf{a}}\cdot\tilde{\mathbf{c}}.
\end{aligned} \qquad \text{(C6)}$$

We can further make use of[38]

$$\tilde{\mathbf{c}}\cdot\tilde{\mathbf{a}}\overline{\otimes^n\tilde{\mathbf{c}}} = \tilde{\mathbf{a}}\cdot\overline{\otimes^{n+1}\tilde{\mathbf{c}}}+\frac{n}{2n+1}\tilde{\mathbf{a}}\cdot\boldsymbol{\Delta}^{(n)}\odot^{n-1}\overline{\otimes^{n-1}\tilde{\mathbf{c}}}, \qquad \text{(C7)}$$

and similar relationships to directly read off the coefficients $\boldsymbol{\alpha}$ defined through

$$f(\mathbf{c}+\mathbf{a}) = f_0(\mathbf{c})\sum_{n,i} \tilde{c}^{2i}\boldsymbol{\alpha}_{n,i}(\mathbf{a})\odot^n(\otimes^n\overline{\tilde{\mathbf{c}}}) \tag{C8}$$

by comparing (C5) with (C8). Notice that for the case $n \leqslant 1$ which covers Grad's 13th moment approximation, one can remove the anisotropic $\overline{\cdots}$ symbols in (C5).

[1] M. Hütter and M. Kröger, J. Chem. Phys. **124**, 044511 (2006).
[2] O. Dupont, F. Dubois, and A. Vedernikov, Meas. Sci. Technol. **11**, 331 (2000).
[3] F. Zheng, Adv. Colloid Interface Sci. **97**, 253 (2002).
[4] A. Melling, Meas. Sci. Technol. **8**, 1406 (1997).
[5] A. Pérez-Madrid, J. M. Rubí, and P. Mazur, Physica A **212**, 212 (1994).
[6] J. M. Rubí and P. Mazur, Physica A **250**, 253 (1998).
[7] L. Waldmann, in *Thermodynamik der Gase*, Handbuch der Physik, Vol. 12, edited by S. Flügge (Springer, Berlin, 1958), p. 373.
[8] P. S. Epstein, Proc. Phys. Soc. London **47**, 259 (1945).
[9] E. A. Mason and S. Chapman, J. Chem. Phys. **36**, 627 (1962).
[10] J. Fernández de la Mora, J. Aerosol Sci. **33**, 477 (2002).
[11] J. Fernández de la Mora and J. M. Mercer, Phys. Rev. A **26**, 2178 (1982).
[12] I. Goldhirsch and D. Ronis, Phys. Rev. A **27**, 1616 (1983).
[13] J. Fernández de la Mora and D. E. Rosner, J. Fluid Mech. **125**, 379 (1982).
[14] B. E. Dahneke, J. Aerosol Sci. **4**, 139 (1973).
[15] M. L. Laucks, G. Roll, G. Schweiger, and E. J. Davis, J. Aerosol Sci. **31**, 307 (2000).
[16] B. E. Dahneke, J. Aerosol Sci. **4**, 147 (1973).
[17] H. J. Keh and C. L. Ou, Aerosol Sci. Technol. **38**, 675 (2004).
[18] H. J. Keh and H. J. Tu, Colloids Surf., A **176**, 213 (2001).
[19] J. Fernández de la Mora, Phys. Rev. A **25**, 1108 (1982).
[20] M. Kröger and M. Hütter, Comput. Phys. Commun. (in press).
[21] P. García-Ybarra and D. E. Rosner, AIChE J. **35**, 139 (1989).
[22] H. C. Öttinger, *Beyond Equilibrium Thermodynamics* (Wiley, Hoboken, NJ, 2005).
[23] X. Chen, J. Phys. D **33**, 803 (2000).
[24] H. Brenner and J. R. Bielenberg, Physica A **355**, 251 (2005).
[25] F. Zheng and E. J. Davis, J. Aerosol Sci. **32**, 1421 (2001).
[26] L. Waldmann, Z. Naturforsch. A **14**, 589 (1959).
[27] Y. Sone, *Kinetic Theory and Fluid Dynamics, Modeling and Simulation in Science, Engineering and Technology* (Birkhäuser, Boston, 2002).
[28] L. Waldmann, in *Rarefied Gas Dynamics*, Proceedings of the Second International Symposium on Rarefied Gas Dynamics, edited by L. Talbot (Academic, New York, 1961), pp. 323–344.
[29] H. Rohatschek and W. Zulehner, J. Colloid Interface Sci. **119**, 378 (1987).
[30] S. Hess, in *Vielteilchensysteme*, Bergmann-Schaefer, Lehrbuch der Experimentalphysik, Vol. 5 (W. de Gruyter, Berlin, 1992), p. 41.
[31] A. N. Gorban and I. V. Karlin, Physica A **360**, 325 (2006).
[32] H. Struchtrup and M. Torrilhon, Phys. Fluids **15**, 2668 (2003).
[33] S. Ansumali, I. V. Karlin, and H. C. Öttinger, Europhys. Lett. **63**, 798 (2003).
[34] A. N. Gorban and I. V. Karlin, Physica A **206**, 401 (1994).
[35] S. S. Chikatamarla, S. Ansumali, and I. V. Karlin, Europhys. Lett. **74**, 215 (2006).
[36] S. Chapman and T. G. Cowling, *The Mathematical Theory of Non-Uniform Gases*, 3rd ed. (Cambridge University Press, Cambridge, 1970).
[37] L. E. Reichl, *A Modern Course in Statistical Physics* (Wiley, New York, 1998).
[38] M. Kröger, *Models for Polymeric and Anisotropic Liquids*, Lecture Notes in Physics Series, Vol. 675 (Springer, Berlin, 2005).
[39] M. Kröger, Phys. Rep. **390**, 453 (2004).
[40] The expression for $\mathbf{F}[\langle\phi_0^2\rangle,\tilde{\mathbf{c}}_T]$ corrects our previous result for a force contribution presented in Ref. 1.
[41] A. Einstein, Z. Phys. **27**, 1 (1924).
[42] F. Zheng, Adv. Colloid Interface Sci. **97**, 255 (2002).
[43] S. K. Friedlander, *Smoke, Dust and Haze* (Wiley, New York, 1997).
[44] P. G. Saffman, J. Fluid Mech. **22**, 385 (1965).
[45] P. G. Saffman, J. Fluid Mech. **31**, 624 (1968).
[46] C.-T. Wang, AIAA J. **10**, 713 (1972).
[47] S. G. Ivanov and A. M. Yanshin, Fluid Dyn. **15**, 449 (1980).
[48] S. N. Semenov and M. E. Schipf, Phys. Rev. E **72**, 041202 (2005).
[49] Our expressions for $\mathbf{F}[1,\tilde{\mathbf{c}}_T]$ and $\mathbf{F}[\langle\phi_1^1\rangle]$ are both smaller by a factor of $\sqrt{\pi}$ than the results of Garcia-Ybarra and Rosner Ref. 21. If their expressions are evaluated in the sphere limit, their results also seems to differ by $\sqrt{\pi}$ from Waldmann (Refs. 26 and 28), while we recover Waldmann's (correct) expressions exactly.
[50] J. R. Dorfman and J. V. Sengers, Physica A **134**, 283 (1986).
[51] M. Kröger and H. S. Sellers, J. Chem. Phys. **103**, 807 (1993).
[52] J. Honerkamp, *Stochastic Dynamical Systems* (Wiley, New York, 1993).
[53] H. C. Öttinger, *Stochastic Processes in Polymeric Fluids* (Springer, Berlin, 1996).
[54] M. Hütter and H. C. Öttinger, J. Chem. Soc., Faraday Trans. **94**, 1403 (1998).
[55] A few minus signs in front of terms containing Z_k and $\mathbf{\Pi}\cdot\mathbf{n}$ were misprinted in Ref. 1, but actually had no effect on the results. The current manuscript should correct these misprints.